Supplementary Information (SI) for Chemical Science.
This journal is © The Royal Society of Chemistry 2025

Supplementary Information

Rational Design of Gold Nanoparticle-based Chemosensors for Detection of the Tumor Marker 3-methoxytyramine

Sebastian Franco-Ulloa,[‡,a,b] Andrea Cesari,[‡,c,d] Giordano Zanoni,[‡,c] Laura Riccardi,[a] Joseph Wallace,[a,c] Beatrice Bernadette Mascitti,[c] Federico Rastrelli,[c] Fabrizio Mancin*[,c] and Marco De Vivo*[,a]

a) Molecular Modeling and Drug Discovery, Istituto Italiano di Tecnologia, via Morego 30, 16163 Genova, Italy
b) Expert Analytics, Møllergata 8, 0179 Oslo, Norway
c) Department of Chemical Science, University of Padova, Via Marzolo 1, 35131 Padova, Italy
d) Department of Chemistry and Industrial Chemistry, University of Pisa, via Moruzzi 13, 56124 Pisa, Italy
‡) these authors contributed equally

Table of Contents

Computational Materials and Methods 3

Experimental Materials and Methods 6

Computational Supplementary Results 11

Experimental Supplementary Results 20

Supplementary References 63

Computational Materials and Methods

Query of the PDB Database

The PDB database (https://www.rcsb.org/) was queried to fetch all the structures that were elucidated with a catecholamine derivative as a standalone guest. We looked for any of the 13 molecules in the biosynthetic pathways of catecholamines and trace amines (Figure S1). The PDB ID of such molecules were 1WE, 3MT, AEF, ALE, DAH, LDP, LNR, NMT, PEA, PHE, OTR, SYP, and TYR. A complete list of the PDB codes associated with each guest can be found in Table S1. The full query for 3-MT was: "Comp Id (Nonpolymer Entity Instance Container Identifiers) = "3MT" AND (Comp Id (Nonpolymer Instance Feature Summary) NOT EXISTS OR Comp Id (Nonpolymer Instance Feature Summary) NOT = "3MT" OR Feature Type NOT = "HAS_COVALENT_LINKAGE")." Lastly, a binding pocket was defined as the collection of standard amino acids with at least one heavy (i.e., non-hydrogen) atom within 0.5 nm of the guest molecule.

Molecular Modeling

The NanoModeler webserver[1,2] was used to generate the initial conformation of the AuNPs (Figure 1). This server produces 3D structures with the coating ligands in an extended conformation. In this study, we used 2 nm AuNPs coated by 60 thiols (i.e., $Au_{144}(SR)_{60}$). NanoModeler also produces the corresponding parameters files for the AuNPs. The inner quasi-static gold atoms of the AuNPs were modeled as neutral spheres with van der Waals parameters taken from Heinz et al.,[3] and the staple-like motifs at the gold-sulfur interface were modeled with the AMBER-compatible parameters derived by Pohjolainen, et al.[4] For the outer monolayer, PROPKA-v3.1[5] was used to determine the most probable protonation state of a single stretched ligand at a neutral pH. The atomic partial charges were derived with the restrained electrostatic potential (RESP) method[6] with the ligand in a fully extended conformation with bonded parameters taken from the Generalized Amber Force Field (GAFF).[7]

The starting structure of each AuNP-analyte dyad included ten copies of the analyte. Previous fluorometric titration experiments showed that 2 nm AuNPs can bind up to 30 analyte molecules each.[8] Thus, using ten analyte molecules in our simulations ensured that the monolayer remained undersaturated. The analytes were initially placed two-thirds of the way into the monolayer using in-house scripts written in Python. That is, the distance between each analyte's center of mass (COM) and the gold core's surface was one-third of the total length of the coating ligands. The initial orientation of the analytes was determined randomly but reproducibly (i.e., with a random seed) and ensured a minimum distance of 0.15 nm between atoms to avoid intermolecular clashes. The analytes were parametrized as the coating thiols, using PROPKA-v3.1,[5] the RESP method,[6] and the GAFF force field[7] to obtain the protonation state, partial charges, and force-field parameters, respectively.

After generating models for the AuNPs and the analytes, their structure (and parameters) files were merged into a single system. A dodecahedral simulation box was defined around the system leaving a minimum distance of 1.6 nm between the AuNP and the box's faces. Then, the box was solvated with TIP3P water molecules.[9] Sodium chloride was added to reach electroneutrality and a salt concentration of 150 mM, a typical ionic strength in biological fluids. The fully solvated system was minimized with the steepest descent method for a maximum of 50,000 steps. All the simulations in this study employed periodic boundary conditions, an integration timestep of 2 fs, linear constraints on all bonds involving hydrogen atoms,[10] and a cutoff radius of 1.2 nm for short-ranged nonbonded interactions. The simulations also accounted for long-ranged electrostatic interactions using the fourth-ordered particle-mesh Ewald method.[11] The simulations in this study were run in Gromacs-v2018.3,[12] and the trajectory files were analyzed with in-house scripts using the MDAnalysis-v1.0 Python open library.[13]

Steered Molecular Dynamics Simulations

Following system minimization, the coating monolayers were allowed to equilibrate around the embedded analyte molecules. To this end, the systems were thermalized and pressurized while restraining each analyte's atoms with a harmonic potential (k_b = 10,000 kJ mol^{-1} nm^{-2}). The thermalization step consisted of a 500-ps-long simulation in the NVT statistical ensemble that heated the system to 300 K, at a constant rate, using a velocity-rescale thermostat (τ_B = 0.1 ps). The pressurization was another 500-ps-long simulation in the NPT statistical ensemble that equilibrated the pressure to 1 bar using a Berendsen barostat (τ = 2.0 ps, $\kappa = 4.5 \times 10^{-5}$ bar^{-1}).

Once the systems reached the target temperature and pressure, they were subject to a steered MD simulation in which each analyte was simultaneously pulled away from the AuNP's COM. A harmonic potential (k_{bias} = 2,000 kJ mol^{-1} nm^{-2}) coupled the COM of each analyte to the COM of the AuNP (i.e., r_{COM}). The equilibrium value of the steering potential increased at a rate of 0.4 nm ns^{-1}. This increased rate allowed the unbinding to occur within 10 ns (for ligands 2-nm-long when extended). Notably, for spherical AuNPs, each analyte molecule served as an individual replica of the overall unbinding process.

Hardware/Software Performance for Steered Simulations.

Each system, consisting of an Au_{144} gold core; 60 covalently bound ligands; 10 analytes; water; and counterions, underwent simulation on a single computational node equipped with 36 cores featuring an Intel Xeon E5-2630 CPU. Across the 100 simulations of the test set, steered molecular dynamics simulation demonstrated an average performance of 22.74 ± 0.94 ns per day.

Binding Score

During the steered MD simulations, the force acting on the collective variable, r_{COM} ,was stored every 4 ps and used to reconstruct the PMF profile along r_{COM} . Then, a binding score, W, was estimated using Equation S1, where $\langle F(r_{COM})\rangle$ is the force along the collective variable, r_{COM} (averaged over the ten analyte molecules), and r_{COM}^{best} is the distance at which the analyte is the most stable inside the monolayer (F closest to zero). In practice, the integral in Equation S1 extended to half the length of the shortest box edge.

$$W = -\left|\int_{r_{COM}^{best}}^{\infty}\langle F(r_{COM})\rangle r_{COM}\right| \qquad \text{(Equation S1)}$$

All the scores reported in this work correspond to the median score W of all the analyte molecules, and the associated uncertainty is the unbiased standard error.

Training Set Adjustment

The method was further calibrated by combining the binding scores, W , of the training set with the experimentally available binding energies Figure S2. Our computational protocol resulted in affinity scores, W , spanning from -3.60 ± 0.55 to -20.90 ± 1.48 kcal mol^{-1}. Even if this represents a larger range than that of the experimental binding affinities, a linear regression showed that the binding score values and the binding free energies of the 22 dyads of the training set with available experimental affinity (ΔG_{exp}) had a correspondence, given by Equation S2 (r^2 = 0.49). Indeed, the ratio between the score, W , and free energy, $\frac{\Delta G_{exp}}{W} = 0.60$, was constant throughout all the dyads (Figure S2 inset).

$$\Delta G = 0.26 \times W - 3.78\ kcal\ mol^{-1} = W_{adj} \quad \text{(Equation S2)}$$

The agreement between the calculated and experimental affinities was less satisfactory in the case of dyads with not-measurable affinity. However, eight out of nine of them were assigned to the low end of the calculated affinities range (>-12 kcal mol^{-1}), confirming the correlation between calculated and experimental affinities. It should also be pointed out that measuring low affinities is experimentally difficult and consequently dyad classification might be affected by errors when distinguishing between low affinity and affinity below the measurable limit.

Equation S2 was subsequently used to calculate an adjusted binding score, W_{adj}, for the AuNP library of 3-MT hosts.

Experimental Materials and Methods

Methods

All the NMR experiments were performed at 25 °C on a Bruker AVANCE III spectrometer operating at 500.13 MHz ^{1}H and 125.8 MHz ^{13}C Larmor frequencies and equipped with a 5 mm z-gradient broad-band inverse (BBI) non-cryogenic probe.

High-power water saturation transfer difference (HPwSTD), experiments were performed using a previously described pulse sequence.[14] DOSY 2D maps were obtained by means of a LED-BPP (ledbpgp2s) pulse sequence. Each spectrum was processed with both Topspin 3.1 and Dynamics Center 2.2.1 (Bruker BioSpin GmbH, 2014). Diffusion coefficients were extracted from fits of the peak intensities versus gradient strengths using the equation

$$I_G = I_{G0} \exp\left(-(\gamma \delta G)^2 D\left(\Delta - \frac{\delta}{3} \right) \right)$$

where I_{G0} is the signal intensity in the absence of the gradient spin-echo, G the gradient strength, D the diffusion coefficient, Δ the diffusion delay, δ the length of the gradient pulses and γ the magnetogyric ratio of the observed nuclide. Inverse Laplace transform was also performed on the data to check for possible multimodal signal decays.

High Resolution mass spectra (HRMS) were obtained with a Waters Xevo G2.S (Q-TOF) mass spectrometer (MeOH, 0.5% formic acid).

UV-Vis spectra were recorded with Agilent Cary 50 and Cary 100 spectrophotometers.

The hydrodynamic sizes (Dynamic Light Scattering, DLS) and ζ-potentials were measured with a Malvern Zetasizer Nano-S equipped with a HeNe laser (633nm) and a Peltier thermostatic system. Measurements were performed at 25 °C in water or PBS mM buffer at pH 7.

Transmission electron microscopy (TEM) images were recorded with a Jeol 300 PX electron microscope. A drop of a 0.5 mg/mL dispersion of gold nanoparticles in methanol was deposited on the sample grid. The droplet was then dried with the aid of a piece of paper. TEM images were analysed with the ImageJ® software package.

Thermogravimetric analysis (TGA) was performed with a Q5000 IR model TA. Typically, 50 μL of the stock solution (in D_2O) was placed in a platinum high-temperature crucible and it was evaporated to constant weight at 80 °C in air. Then a 10 °C/min heating program from 100 °C to 1000 °C was applied under air flow. The weight loss was calculated from the initial point after the drying treatment (which

also allows to confirm the concentration of the stock solution) and the final one after the complete burning of the organic component at 850 °C.

Ligands Synthesis

General. All solvents and reactants were purchased by Merck or Iris Biotech and used as received without further purification. Reactions were monitored by thin layer chromatography (TLC) developed on 0.25 mm Merck silica gel plates (60 F254). Chromatographic purifications were performed using Macherey-Nagel silica gel 60 (70-230 mesh).

Abbreviations:

AA: amino acid

2-CTC: 2-chlorotrityl chloride

DCM: dichloromethane

DIPEA: diisopropylethylamine

DMF: dimethylformamide

Fmoc: fluorenylmethyloxycarbonyl

HBTU: hexafluorophosphate benzotriazole tetramethyl uranium

HFIP; hexafluoroisopropanol

MeOH: methanol

MeOD: deuterated methanol (CD_3OD)

Synthesis Procedure. Tripeptide ligands were synthesized by solid phase synthesis using commercial Fmoc protected amino acids and 8-thioacethyloctanoic acid. The 8-thioacethyloctanoic was synthesized as follows (Scheme S1):

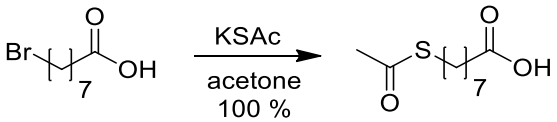

Scheme S1. 8-thioacethyloctanoic synthesis.

8-bromooctanoic acid (1.50 g, 6.72 mmol, 1 equiv.) and potassium thioacetate (1.15 g, 10.1 mmol, 1.5 equiv.) were added to dry acetone (50 mL) and stirred at 35 °C overnight. The solvent was evaporated under reduced pressure and water (30 mL) was added to the residue. The mixture was then extracted

with 3 x 30 mL DCM and the product was purified by flash column chromatography on silica (eluent: DCM/MeOH 95/5). The product (1.472 g, yield = 100 %) was collected as a beige solid.

^{1}H NMR (500 MHz, $CDCl_3$) δ: 2.67 (t, J = 7.3 Hz, 2H, CH_2S), 2.16 (t, J = 7.5 Hz, 2H, CH_2COOH), 2.13 (s, 3H, CH_3S), 1.44 (p, J = 8.3, 7.8 Hz, 2H, CH_2CH$_2$S), 1.37 (m, 2H, CH_2CH$_2$COOH), 1.22 – 1.11 (m, 6H, CH_2).

^{13}C NMR (126 MHz, $CDCl_3$) δ 195.57 (*C*OS), 179.45 (*C*OOH), 33.78 (*C*H$_2$), 30.30 (*C*H$_3$S), 29.29 (*C*H$_2$), 28.83 (*C*H$_2$), 28.69 (*C*H$_2$), 28.56 (*C*H$_2$), 28.38 (*C*H$_2$), 24.40 (*C*H$_2$).

The general procedure (Scheme S2) for ligands synthesis is described in the following paragraphs. Detailed characterization of each ligand is reported thereafter.

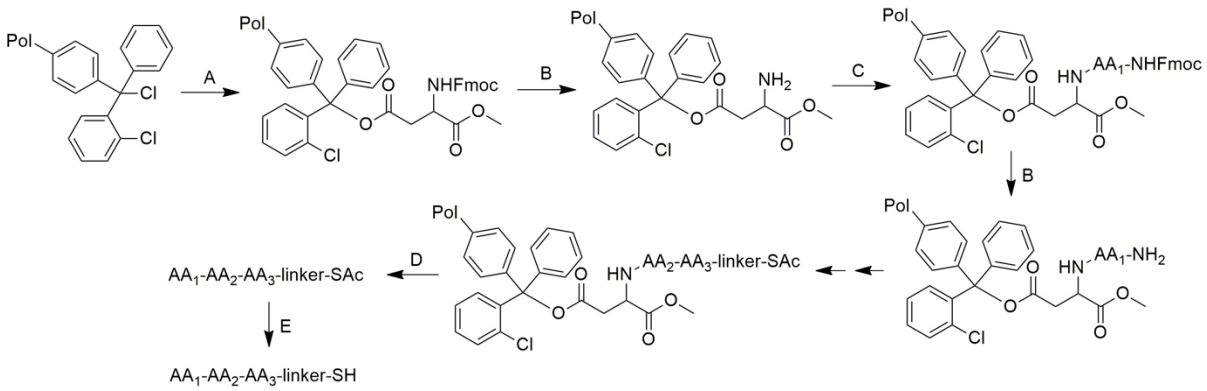

Scheme S2. Synthetic scheme for the tripeptide-thiols. A) DIPEA, DMF, FMOC-L-Asp-OMe; B) 4-methylpiperidine, DMF; C) Fmoc-L-AA-OH, HBTU, DIPEA, DMF; D) HFIP, DCM; E) NaOMe, MeOH, Amberlyst 15 H^+ resin.

2-CTC resin was swelled under agitation in dry DMF for 1h, excess DMF was then removed without completely drying the resin.

First Amino Acid Loading and Deprotection. To the pre-swelled 2-CTC resin (loading = 1,35 mmol/g, 400 mg, 0.54 mmol, 1 equiv.) were sequentially added dry DMF (9 mL), DIPEA (0.8 mL, 4.59 mmol, 5.3 equiv.) and then Fmoc-L-Asp-OMe (320 mg, 0.87 mmol, 1.6 equiv.). The mixture was stirred at room temperature overnight. The resin was filtered and washed with 3 x 6 mL dry DMF. Subsequently, to cap unreacted CTC residues, dry DCM (7 mL), dry MeOH (7 mL) and DIPEA (0.5 mL) were added to the resin and the mixture was left under stirring for 1 h. The solution was then removed by filtration and the resin washed with 3 x 6 mL dry DCM.

20% 4-methylpiperidine in DMF (7 mL) was then added to the resin, the mixture was stirred for 5 minutes and then the solvent was removed by filtration. This procedure was repeated a second time and then the resin was washed with 3 x 6 mL DMF.

Second and Third Amino Acid Coupling. The desired Fmoc-L-AA-OH (1.08 mmol, 2 equiv.) was dissolved in dry DMF (2 mL) in a glass vial, DIPEA (376 μL, 4 equiv.) and HBTU (409 mg, 2 equiv.) were then added to the solution. The mixture was manually stirred for 5 minutes and then added to the resin. The mixture was left under stirring at room temperature for 3 h for the second amino acid or 7 h for the third one. The resin was then filtered and washed with 3 x 6 mL dry DMF.

Linker Coupling. 8-(acetylthio)octanoic acid (236 mg, 1.08 mmol, 2 equiv.) was added to a glass vial, followed by dry DMF (2 mL), DIPEA (376 μL, 4 equiv.) and HBTU (409 mg, 2 equiv.). The mixture was manually stirred for 5 minutes and then added to the resin. The mixture was left under stirring at room temperature overnight. The resin was then washed with 3 x 6 mL dry DMF and 3 x 6 mL dry DCM.

Resin Cleavage. 20% hexafluoroisopropanol (HFIP) in dry DCM (8 mL) was added to the resin and left under stirring at room temperature for 1 h. The liquid was recovered and evaporated. This step was repeated a second time. The resin was then washed with 3 x 6 mL DCM. All the filtrate was combined and evaporated under reduced pressure.

Thiol Deprotection. The desired tripeptide-linker-SAc (0.185 mmol, 1 equiv.) was added to a 5 mL round bottom flask under nitrogen atmosphere. Dry MeOH (2 mL) and sodium methoxide (30 mg, 0.555 mmol, 3 equiv.) were then added and the mixture was stirred for 2 h at room temperature. A small amount of Amberlyst 15 hydrogen form resin was then added to the solution and left standing for 20 min at room temperature. The resin was removed by filtration and the filtrate was evaporated under reduced pressure. The obtained product was used as obtained without further purification.

N-Boc Deprotection. In the case of peptide ligands featuring N-Boc protected side chains, to the already thiol-deprotected species50% TFA in DCM (4 mL) was added. The solution was left under stirring for 30 minutes and then evaporated under reduced pressure. The obtained product was used as obtained without further purification.

Nanoparticles Synthesis

The nanoparticles were syntheses according to previously published procedures as follows. A solution of $HAuCl_4 \cdot 3H_2O$ (50 mg, 0,13 mmol, 1 equiv.) in 0.5 mL of milliQ H_2O was extracted with a solution of tetraoctylammonium bromide (172 mg, 0.31 mmol, 2.5 equiv.) in toluene (125 mL). The solution was poured in a 250 mL round bottom flask under nitrogen atmosphere and dioctylamine (755 μL, 2.5

mmol, 20 equiv.) was added. The solution was stirred for 2 h and then placed in an ice bath. A solution of $NaBH_4$ (47 mg, 1.3 mmol, 10 equiv.) in ultrapure H_2O (0.5 mL) was added and the dispersion was left under stirring for 2h. The water was removed with the aid of a separating funnel and the toluene phase was transferred back to a 250 mL round bottom flask in an ice bath under nitrogen atmosphere. A solution of the desired thiol (0.123 mmol, 2.5 equiv.) in methanol (0.5 mL) was then added and the colloid was kept under stirring overnight. The suspension was then centrifuged (5 min at 5000 rpm) and the nanoparticles were dispersed in ca. 2 mL of MeOH, sonicated with an ultrasonic bath and precipitated with diethyl ether. To collect the nanoparticles the dispersion was centrifuged for 5-8 min at 5000 rpm. This washing step was repeated three times. The nanoparticles were then purified three times by size exclusion chromatography on Sephadex LH-20 in methanol. The nanoparticles were then dried in vacuum and stored dry or as a 20 mM water stock solution in a freezer at -20 °C.

Average nanoparticles formulas were calculated by the TEM and TGA data using the spherical approximation for the gold cores.

Computational Supplementary Results

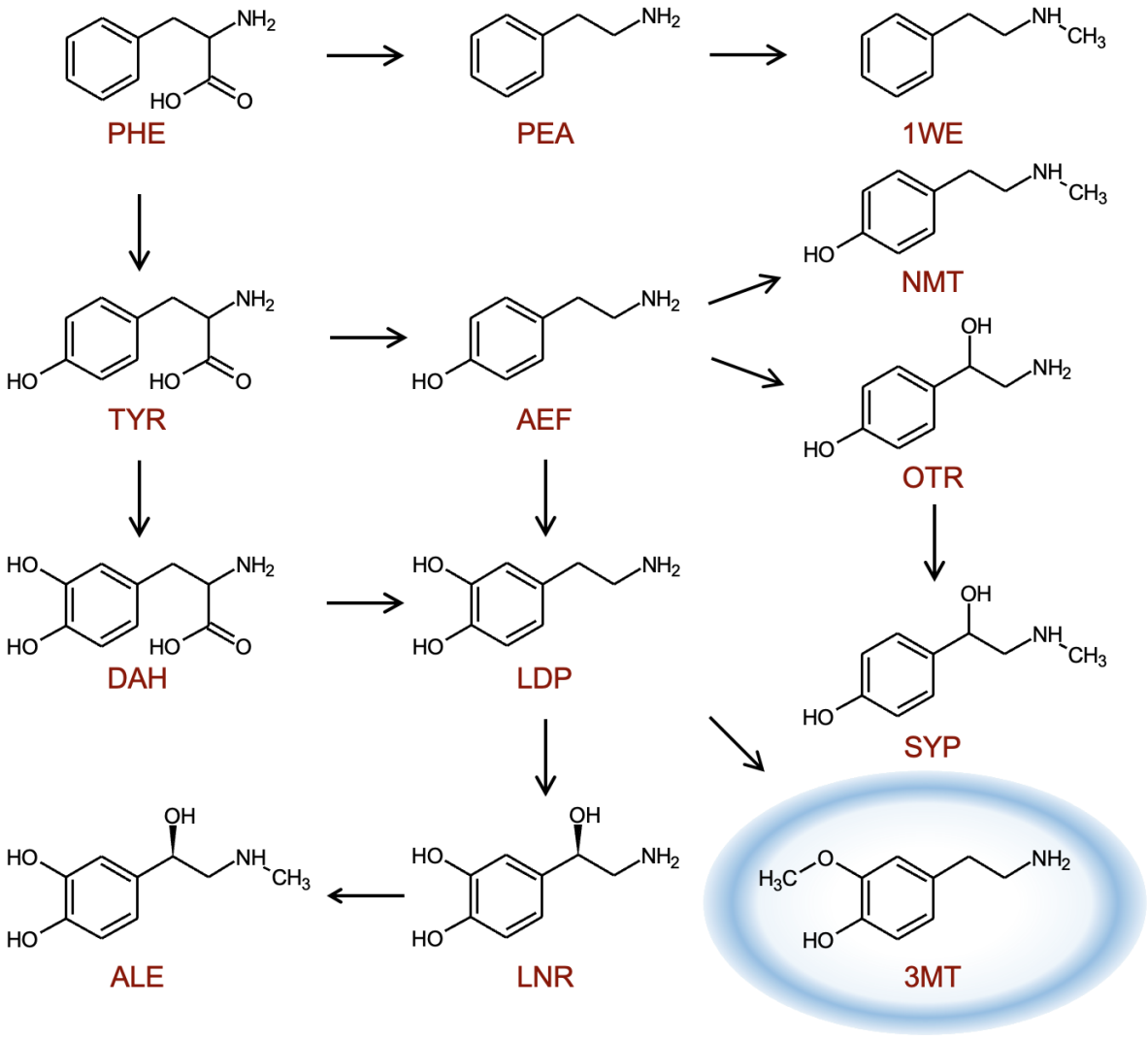

Figure S1. Biosynthetic pathways of catecholamines and trace amines. Each molecule is paired with its PDB ID.

Table S1. PDB IDs used for the analysis of the binding pockets of catecholamines and trace amines. The structures are grouped by guest.

Guest Molecule PDB ID	Number of Structures	PDB Structures ID
1WE	3	4LAR, 4XP9, 8JSO
3MT	1	1AEB
AEF	4	3BRA, 4N7C, 5FF9, 8EEK
ALE	6	2HKK, 4A7U, 4LDO, 7BRN, 7BTS, 8THL
DAH	6	3TEG, 3TEH, 4P6S, 6JU9, 6ON3, 6PAH
LDP	24	2A3R, 2QMZ, 2VQ5, 3NK2, 4A7V, 4DTZ, 4DU2, 4DUB, 5LOG, 5PAH, 5PHH, 6DYO, 6ZN2, 7CKZ, 7F0T, 7F1O,

		7F1Z, 7F23, 7F24, 7LJD, 7PIM, 7X2F, 8EEG, 8EEJ
LNR	7	2QEO, 3DYE, 3HCD, 4PAH, 4Y4J, 6M0Z, 6M2R
NMT	0	
OTR	6	1RG2, 1RGT, 2AN4, 3HCA, 3HCE, 8EEF
PEA	13	1D6U, 1D6Y, 1D6Z, 1TNJ, 1UTM, 1UTO, 5GI6, 8IW7, 8IWM, 8J6G, 8W89, 8WC6, 8WCA
PHE	88	1AMU, 1B70, 1C1D, 1F2P, 1I7A, 1IS7, 1IS8, 1KFL, 1OFR, 1OG0, 1USI, 2EFU, 2FMG, 2JB2, 2QMX, 2VBW, 2YPO, 2Z3O, 3AYJ, 3B34, 3BWN, 3CMA, 3CME, 3KGF, 3L4G, 3LKV, 3MK2, 3MWB, 3NUD, 3PCO, 3RZI, 3TCY, 3TD9, 3TK2, 4D2C, 4FXJ, 4IO7, 4JPX, 4JPY, 4PPV, 4TVA, 4UC5, 4UC8, 4UC9, 4XN5, 5CKV, 5CKX, 5CZS, 5CZT, 5D04, 5D05, 5D58, 5D59, 5DCB, 5FII, 5MGH, 5MGU, 5MGW, 5NZK, 5OXN, 6D6N, 6EEI, 6GG4, 6GYP, 6UOB, 6VH5, 6W3V, 6XWM, 6YU3, 6Z80, 7AL9, 7ALB, 7ALC, 7ALZ, 7AM0, 7AQ0, 7AQ9, 7AQA, 7C3J, 7C4N, 7KA0, 7KAB, 7OEX, 7QRI, 7R3B, 7X5J, 8IHR, 8P8X
SYP	0	
TYR	72	1J1U, 1S2K, 1TYA, 1TYB, 1TYD, 1WQ4, 1X8X, 1Y42, 2AMC, 2CSM, 2CYB, 2CYC, 2PV7, 2QAA, 2VBY, 2WHZ, 2XII, 2YPP, 2YPQ, 3B37, 3GGG, 3KDZ, 3MO4, 3O7B, 3PG9, 4CSM, 4GRS, 4HSO, 4OJM, 4OUD, 4P6R, 4PPU, 4QBT, 4R0T, 4TS1, 4WJI, 5CKV, 5CKX, 5DCD, 5IHX, 5IJX, 5JVO, 5T95, 5T9F, 5THH, 5UXN, 5UYY, 6A8Z, 6AGM, 6BQZ, 6EEM, 6EYV, 6HJW, 6HNI, 6IFF, 6JU7, 6JU9, 6L1O, 6OTJ, 6PZ0, 6U60, 6WJO, 6YU7, 7C3L, 7KNX, 7KQR, 7PD1, 7REU, 7RS3, 7UX8, 7VYS, 8DAY

Table S2. Ligands and analytes forming the dyads used as the training set of the computational protocol.

A = Gabrielli, L. et al. Detection and identification of designer drugs by nanoparticle-based NMR chemosensing. Chem. Sci. 9, 4777–4784 (2018)[8]

B = Umpublished results

C = Sun, X., Liu, P. & Mancin, F. Sensor arrays made by self-organized nanoreceptors for detection and discrimination of carboxylate drugs. Analyst 143, 5754–5763 (2018)[15]

D = Sun, X. et al. Molecular-Dynamics-Simulation-Directed Rational Design of Nanoreceptors with Targeted Affinity. Angew. Chemie - Int. Ed. 58, 7702–7707 (2019)[16]

E = Perrone, B., Springhetti, S., Ramadori, F., Rastrelli, F. & Mancin, F. 'NMR chemosensing' using monolayer-protected nanoparticles as receptors. J. Am. Chem. Soc. 135, 11768–11771 (2013)[17]

Ligand Structure	Analyte Structure	Experimental Binding Energy (kcal mol^{-1})	Reference
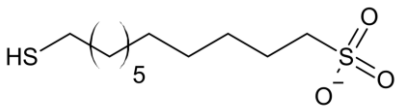	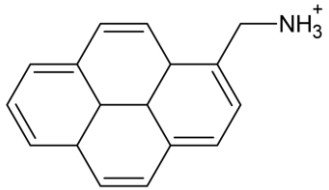	-8.71 ± 0.03	A
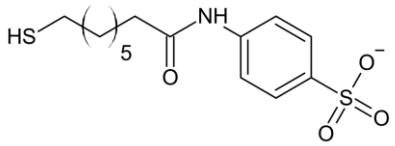	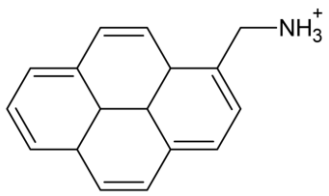	-8.39 ± 0.04	A
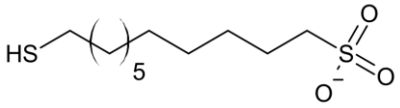	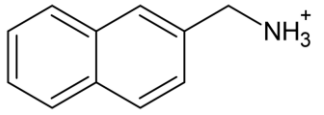	-7.94 ± 0.12	A

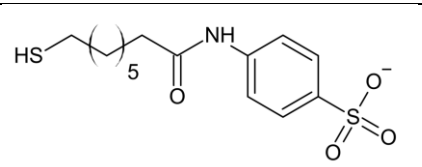	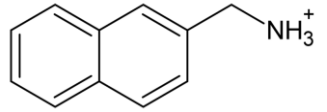	-7.83 ± 0.03	A
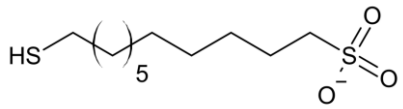	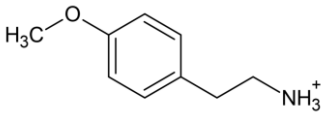	-7.80 ± 0.06	A
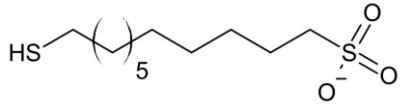	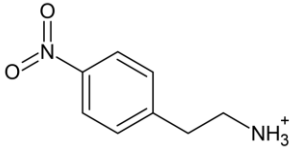	-7.77 ± 0.00	A
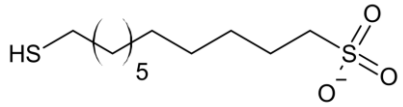	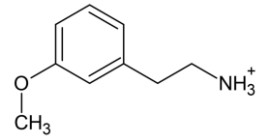	-7.70 ± 0.06	A
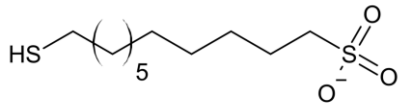	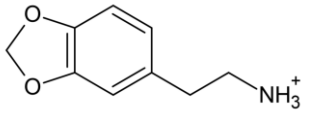	-7.67 ± 0.04	A
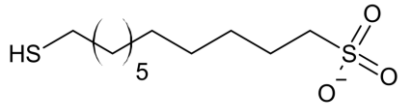	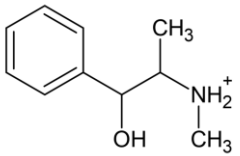	-7.64 ± 0.00	A
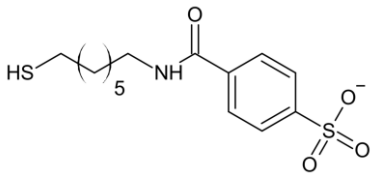	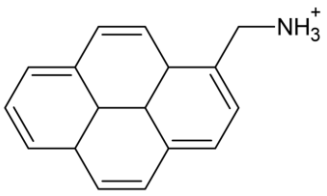	-7.63 ± 0.02	A

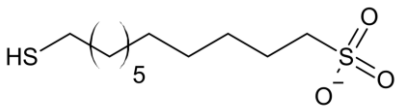	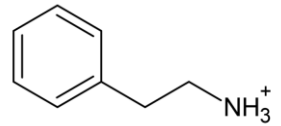	-7.63 ± 0.00	A
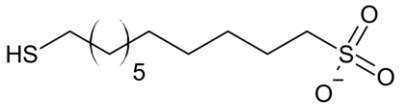	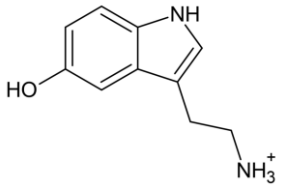	-7.46 ± 0.06	A
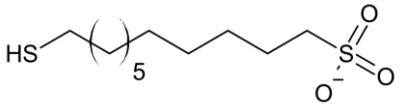	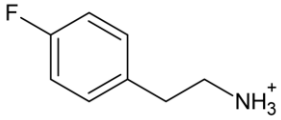	-7.43 ± 0.12	A
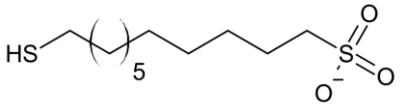	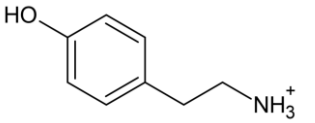	-7.02 ± 0.09	A
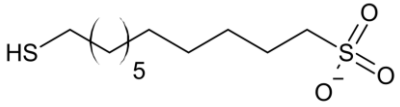	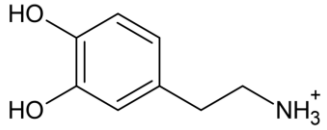	-6.97 ± 0.09	A
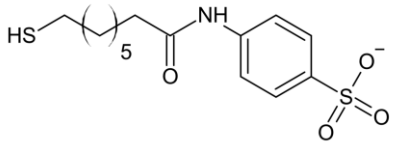	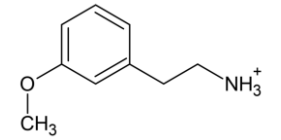	-6.82 ± 0.07	A
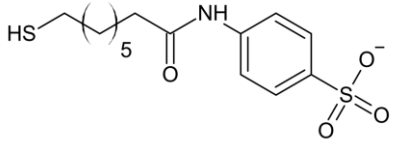	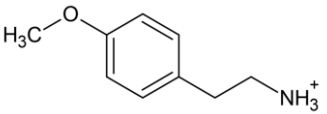	-6.77 ± 0.10	A

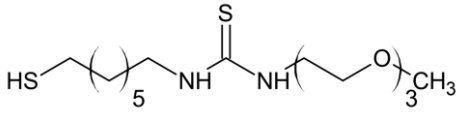	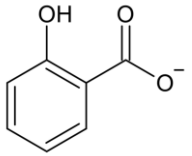	-6.45 ± 0.00	B
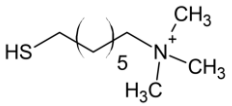	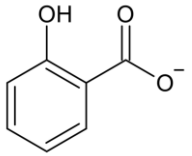	-6.39 ± 0.00	C
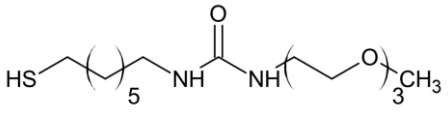	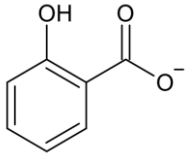	-4.17 ± 0.00	D
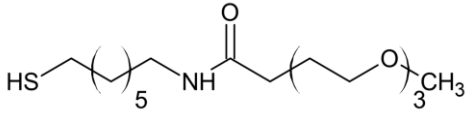	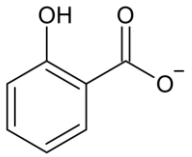	-3.40 ± 0.00	B
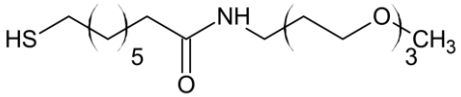	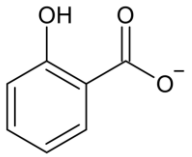	-2.85 ± 0.02	E
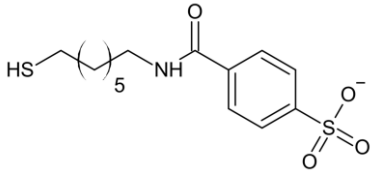	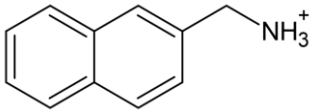	-	A

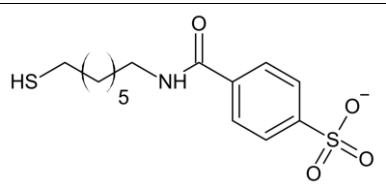	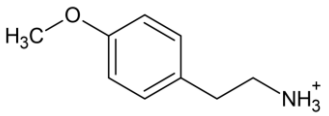	-	A
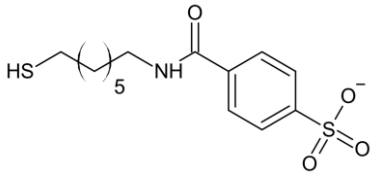	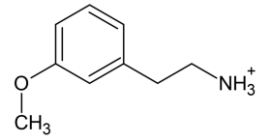	-	A
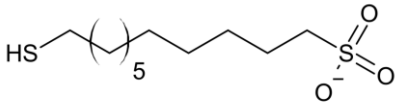	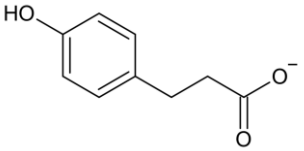	-	A
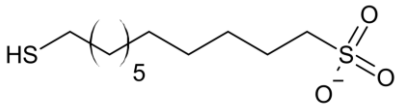	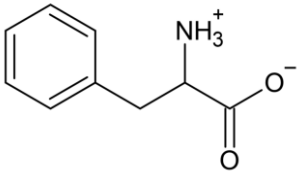	-	A
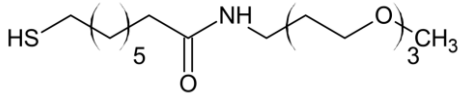	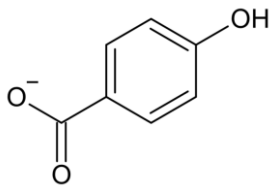	-	D
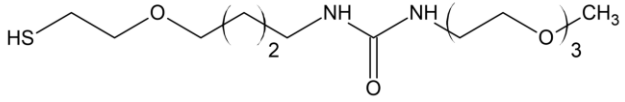	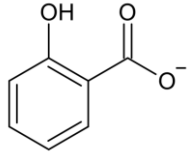	-	D

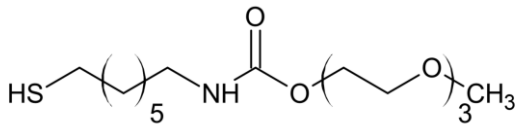	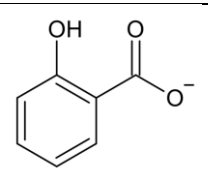	-	B
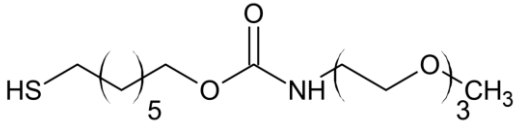	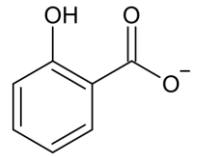	-	D

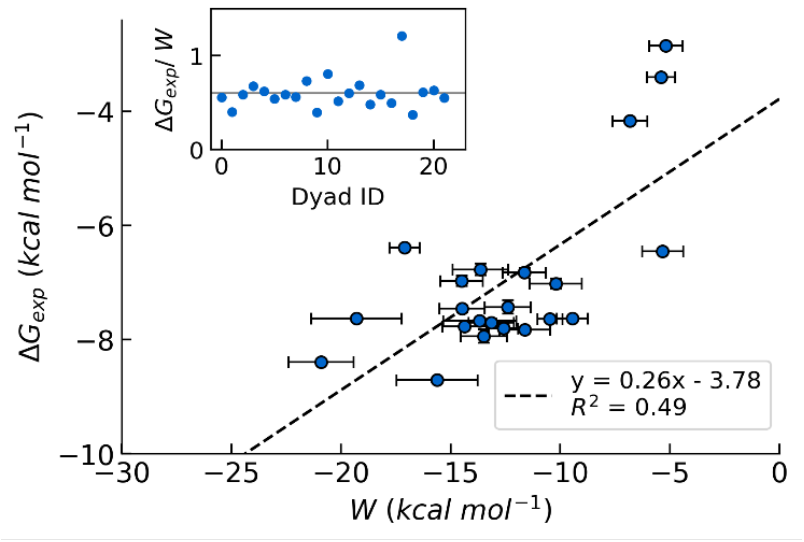

Figure S2. Correlation between the computational binding score, W , and the experimental affinities, ΔG_{exp} for the training database. Inset: Ratios between the computational score and experimental binding energy for the dyads reported in the main figure, in no particular order.

Experimental Supplementary Results

AcS-Trp(Boc)PheAsp

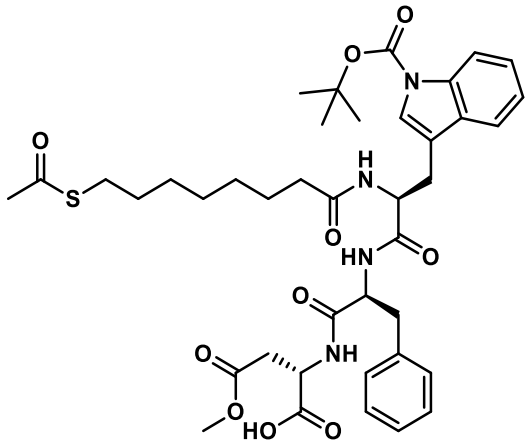

^{1}H NMR (500 MHz, MeOD): δ 8.08 (d, J =7.9 Hz, 1H, C*H* Trp), 7.62 (d, J =7.7 Hz, 1H, C*H* Trp), 7.48 (s, 1H, C*H* Trp), 7.29 – 7.17 (m, 7H, C*H* Trp + C*H* Trp + 5 C*H* Phe), 4.75 – 4.62 (m, 3H, C*H* Trp + C*H* Phe + C*H* Asp), 3.70 (s, 3H, CH_3O), 3.17 – 3.12 (m, 2H, ½ CH_2 Trp + ½ CH_2 Phe), 2.98 – 2.90 (m, 3H, ½ CH_2 Trp + ½ CH_2 Phe + ½ CH_2 Asp), 2.82 – 2.79 (m, 3H, ½ CH_2 Asp + CH_2SAc), 2.23 (s, 3H, CH_3COS), 2.09 (t, J =7.4 Hz, 2H, CH_2CON), 1.66 (s, 9H, CH_3 Boc), 1.47 – 1.39 (m, 4H, 2 CH_2 linker), 1.22 – 1.01 (m, 6H, 3 CH_2 linker).

^{13}C NMR (126 MHz, MeOD): δ 197.60 (*C*OS), 176.16 (*C*=O), 173.97 (*C*=O), 173.41 (*C*=O), 172.91 (*C*=O), 172.59 (*C*=O), 150.98 (*C*=O Boc), 138.09 (quaternary *C* Phe), 136.75 (quaternary *C* Trp), 131.76 (*C*H Phe), 130.47 (*C*H Phe), 129.71 (*C*H Phe), 129.43 (*C*H Phe), 128.58 (quaternary *C* Trp), 127.75 (*C*H Phe), 125.45 (*C*H Trp), 125.17 (*C*H Trp), 123.64 (*C*H Trp), 120.17 (*C*H Trp), 117.54 (quaternary *C* Trp), 116.12 (*C*H Trp), 84.78 (quaternary *C* Boc), 55.65 (*C*H Phe), 54.13 (*C*H Trp), 53.00 (O*C*H$_3$), 50.30 (*C*H Asp), 38.77 (*C*H$_2$ Phe), 36.89 (*C*H$_2$CON), 36.82 (*C*H$_2$ Asp), 30.63 (*C*H$_3$COS), 30.50 (*C*H$_2$ linker), 29.79 (*C*H$_2$SAc), 29.51 (*C*H$_2$ linker), 28.45 (*C*H$_3$ Boc), 28.23 (*C*H$_2$ Trp), 26.67 (*C*H$_2$ linker).

MS-ESI (negative) *m*/*z*: 779.3 ([M]$^-$) (calculated: 779.33).

AcS-TrpPheAsp

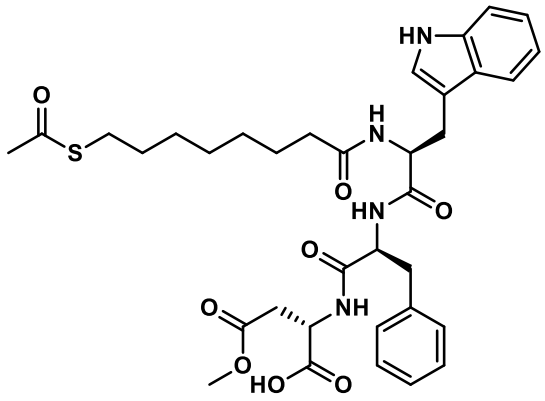

^{1}H NMR (500 MHz, MeOD): δ 8.12 (d, J = 8.2 Hz, 1H, C*H* Trp), 7.62 (d, J = 7.7 Hz, 1H, C*H* Trp), 7.50 (s, 1H, C*H* Trp), 7.33– 7.18 (m, 8H, N*H* + C*H* Trp + C*H* Trp + 5 C*H* Phe), 4.75 – 4.63 (m, 3H, C*H* Trp + C*H* Phe + C*H* Asp), 3.70 (s, 3H, CH_3O), 3.18 – 3.11 (m, 2H, ½ CH_2 Trp + ½ CH_2 Phe), 2.98 – 2.90 (m, 3H, ½ CH_2 Trp + ½ CH_2 Phe + ½ CH_2 Asp), 2.84 – 2.80 (m, 3H, ½ CH_2 Asp + CH_2SAc), 2.28 (s, 3H, CH_3COS), 2.09 (t, J =7.4 Hz, 2H, CH_2CON), 1.49 – 1.35 (m, 4H, 2 CH_2 linker), 1.26 – 1.01 (m, 6H, 3 CH_2 linker).

^{13}C NMR (126 MHz, MeOD): δ 196.34 (*C*OS), 176.30 (*C*=O), 173.77 (*C*=O), 173.50 (*C*=O), 172.99 (*C*=O), 172.54 (*C*=O), 138.09 (quaternary *C* Phe), 135.30 (quaternary *C* Trp), 131.71 (*C*H Phe), 130.48 (*C*H Phe), 129.74 (*C*H Phe), 129.46 (*C*H Phe), 128.61 (quaternary *C* Trp), 127.79 (*C*H Phe), 125.45 (*C*H Trp), 124.56 (*C*H Trp), 123.65 (*C*H Trp), 117.64 (*C*H Trp), 116.25 (quaternary *C* Trp), 115.37 (*C*H Trp), 55.65 (*C*H Phe), 54.19 (*C*H Trp), 53.02 (O*C*H$_3$), 50.24 (*C*H Asp), 38.74 (*C*H$_2$ Phe), 36.83 (*C*H$_2$CON), 36.64 (*C*H$_2$ Asp), 30.66 (*C*H$_3$COS), 30.49 (*C*H$_2$ linker), 29.82 (*C*H$_2$SAc), 29.53 (*C*H$_2$ linker), 28.20 (*C*H$_2$ Trp), 27.71, 26.69 (*C*H$_2$ linker).

MS-ESI (negative) *m*/*z*: 679.2 ([M]$^-$) (calculated 679.28).

HS-TrpPheAsp

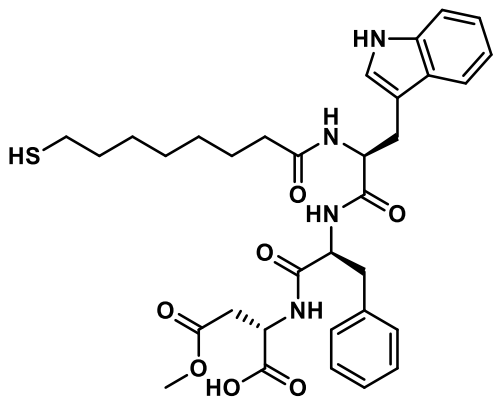

^{1}H NMR (500 MHz, MeOD): δ 7.52 (d, J =7.5 Hz, 1H, C*H* Trp), 7.29 (d, J =7.9 Hz, 1H, C*H* Trp), 7.23–6.95 (m, 9H, N*H* + C*H* Trp + C*H* Trp + C*H* Trp + 5 C*H* Phe), 4.68 (t, 1H, J =5.5 Hz, C*H* Trp), 4.59 (br, 2H, C*H* Phe + C*H* Asp), 3.65 (s, 3H, CH_3O), 3.17 – 3.03 (m, 2H, ½ CH_2 Trp + ½ CH_2 Phe), 2.98 – 2.93 (m, 3H, ½ CH_2 Trp + ½ CH_2 Phe + ½ CH_2 Asp), 2.89 – 2.81 (m, 3H, ½ CH_2 Asp + CH_2SH), 2.07 (t, J =7.1 Hz, 2H, CH_2CON), 1.47 (br, 2H, CH_2 linker), 1.34 (br, 2H, CH_2 linker), 1.22(br, 2H, CH_2 linker), 1.13 (br, 2H, CH_2 linker), 0.98 (br, 2H, CH_2 linker).

^{13}C NMR (126 MHz, MeOD): δ 177.93 (*C*=O), 176.39 (*C*=O), 174.09 (*C*=O), 172.86 (*C*=O), 170.65 (*C*=O), 138.10 (quaternary *C* Phe), 136.45 (quaternary *C* Trp), 131.54 (*C*H Phe), 130.42 (*C*H Phe), 129.53 (*C*H Phe), 129.42 (*C*H Phe), 128.70 (quaternary *C* Trp), 127.73 (*C*H Phe), 124.65 (*C*H Trp), 122.37 (*C*H Trp), 119.73 (*C*H Trp), 119.33 (*C*H Trp), 117.01 (quaternary *C* Trp), 112.38 (*C*H Trp), 55.63 (*C*H Phe), 52.93 (*C*H Trp), 51.47 (O*C*H$_3$), 49.85 (*C*H Asp), 40.11 (*C*H$_2$ Phe), 36.87 (*C*H$_2$CON), 35.08 (*C*H$_2$ Asp), 29.89 (*C*H$_2$S), 29.75 (*C*H$_2$ linker), 29.10 (*C*H$_2$ linker), 28.53 (*C*H$_2$ Trp), 26.57, 24.94 (*C*H$_2$ linker).

MS-ESI (positive) m/z : 661.3 ([M+Na]$^+$) (calculated 661.27).

AcS-TyrProAsp

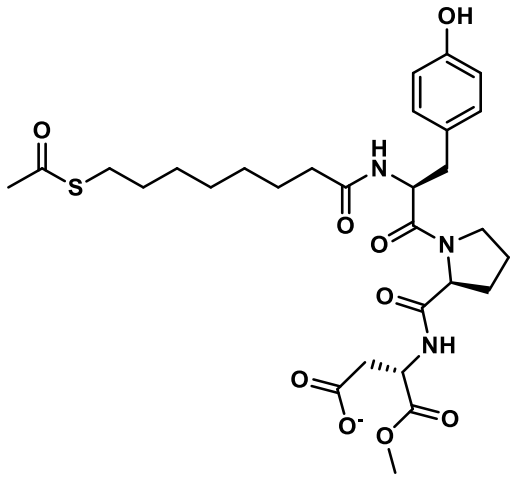

^{1}H NMR (500 MHz, MeOD): δ 7.12 – 7.08 (m, 1H, C*H* Tyr), 7.07 – 7.03 (m, 1H, C*H* Tyr), 6.77 – 6.72 (m, 1H, C*H* Tyr), 6.72 – 6.68 (m, 1H, C*H* Tyr), 4.81 – 4.73 (m, 2H, C*H* Asp + C*H* Tyr), 4.52 – 4.43 (m, 1H, C*H* Pro), 3.87 – 3.77 (m, 2H, NCH_2 Pro), 3.73 (s, 3H, OCH_3 Asp), 3.06 (dd, J = 15.0, 4.8 Hz, 1H, ½ CH_2 Asp), 2.91 (dd, J = 5.7, 2.4 Hz, 1H, ½ CH_2 Tyr), 2.89 – 2.84 (m, 3H, ½ CH_2 Tyr + CH_2SAc), 2.76 (dd, J = 14.3, 9.5 Hz, 1H, ½ CH_2 Asp), 2.30 (s, 3H, CH_3COS), 2.22 – 2.16 (m, 2H, CH_2 Pro), 2.13 (t, J = 7.4 Hz, 2H, CH_2CON), 2.09 – 1.92 (m, 2H, CH_2 Pro), 1.62 – 1.42 (m, 4H, CH_2 linker), 1.41 – 1.10 (m, 6H, CH_2 linker).

^{13}C NMR (126 MHz, MeOD): δ 196.36 (*C*OS), 174.58 (*C*=O), 172.63 (*C*=O), 172.41 (*C*=O), 171.60 (*C*=O), 171.31 (*C*=O), 130.1, 129.8, 127.7, 126.5, 115.0, 114.7 (6C, *C* Tyr), 53.5 (*C*H Pro), 52.4 (*C*H Tyr), 51.1 (O*C*H$_3$ Asp), 48.9 (*C*H Asp), 47.1 (N*C*H$_2$ Pro), 37.8 (*C*H$_2$ Asp), 35.8 (*C*H$_2$ Tyr), 35.4 (*C*H$_2$SAc), 35.2 (*C*H$_2$CON), 29.1 (*C*H$_3$COS), 28.9 (*C*H$_2$ linker), 28.6 (*C*H$_2$ Pro), 25.1 (*C*H$_2$ linker), 24.3 (*C*H$_2$ Pro), 29.1, 28.4, 28.1 (3C, *C*H$_2$ linker).

MS-ESI (negative) *m/z*: 606.2 ([M]$^-$) (calculated 606.25).

HS-TyrProAsp

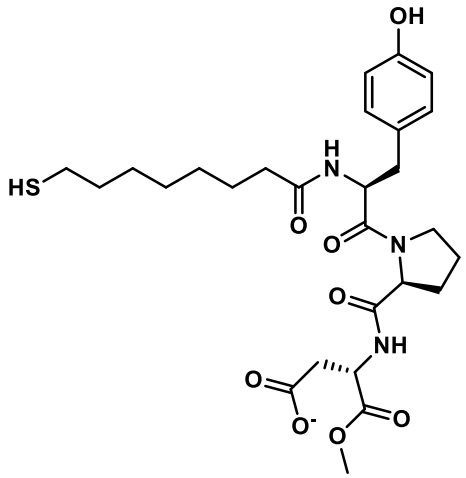

^{1}H NMR (500 MHz, MeOD): δ 6.96 – 6.89 (m, 1H, C*H* Tyr), 6.88 – 6.82 (m, 1H, C*H* Tyr), 6.60 – 6.51 (m, 2H, C*H* Tyr), 4.78 – 4.68 (m, 1H, C*H* Asp), 4.51 – 4.43 (m, 1H, C*H* Pro), 4.42 – 4.35 (m, 1H, C*H* Tyr), 3.82 – 3.67 (m, 1H, NCH_2 Pro), 2.97 (dd, J = 14.6, 6.1 Hz, 1H, ½ CH_2 Asp), 2.89 – 2.55 (m, 3H, ½ CH_2 Asp + CH_2 Tyr), 2.50 – 2.42 (m, 2H, CH_2CON), 2.17 (m, 2H, CH_2SH), 2.11 – 1.94 (m, 2H, CH_2 Pro), 1.94 – 1.83 (m, 2H, CH_2 Pro), 1.77 – 1.46 (m, 4H, CH_2 linker), 1.43 – 1.24 (m, 6H, CH_2 linker).

^{13}C NMR (126 MHz, MeOD): δ 179.94 (*C*=O), 175.71 (*C*=O), 173.53 (*C*=O), 172.94 (*C*=O), 170.51 (*C*=O), 129.9, 129.3, 121.85, 120.9, 118.1, 118.2 (6C, *C* Tyr), 60.5 (*C*H Pro), 53.6 (*C*H Asp), 52.8 (*C*H Tyr), 47.5 (N*C*H_2 Pro), 36.1 (*C*H_2 Tyr), 35.1 (SH*C*H_2), 35.8 (*C*H_2 Asp), 29.1 (*C*H_2CON), 25.1 (*C*H_2 linker), 25.0 (*C*H_2 linker), 28.9, 24.9 (2C, *C*H_2 Pro), 29.3, 28.8, 28.4 (3C, *C*H_2 linker).

HRMS (negative) *m/z*: 564.2368 ([M]$^-$) (calculated 564.2379).

AcS-GlnProAsp

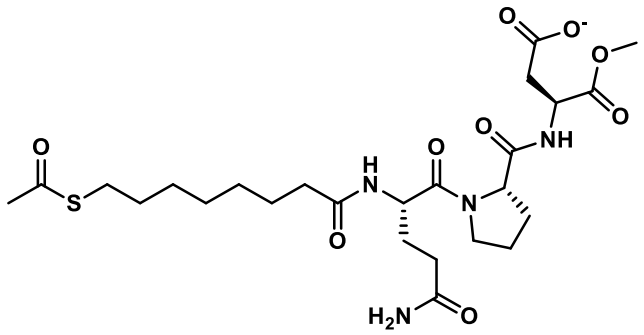

^{1}H NMR (500 MHz, MeOD): δ 4.77 (t, J = 5.8 Hz, 1H, C*H* Asp), 4.63 (t, J = 7.8 Hz, 1H, C*H* Pro), 4.47 (dd, J = 9.2, 4.0 Hz, 1H, C*H* Gln), 3.92 – 3.73 (m, 2H, CH_2N Pro), 3.72 (s, 3H, OCH_3 Asp), 2.93 – 2.79 (m, 4H, CH_2SAc + CH_2 Asp), 2.38 – 2.32 (m, 2H, CH_2CON), 2.30 (s, 3H, CH_3COS), 2.25 – 2.16 (m, 2H, CH_2 Gln), 2.14 – 1.86 (m, 6H, CH_2CO Gln + 2 CH_2 Pro), 1.64 – 1.51 (m, 4H, 2 CH_2 linker), 1.33 – 1.20 (m, 6H, 3 CH_2 linker).

^{13}C NMR (126 MHz, MeOD): δ 196.3 (*C*OS), 176.46 (C=O), 174.74 (C=O), 172.71 (C=O), 172.45 (C=O), 171.34 (C=O), 163.50 (C=O), 59.9 (*C*H Gln), 51.4 (O*C*H$_3$ Asp), 50.3 (*C*H Pro), 48.9 (*C*H Asp), 47.4 (N*C*H$_2$ Pro), 35.3 (*C*H$_2$SAc), 35.1 (*C*H$_2$CON Gln), 29.7 (*C*H$_3$COS), 29.3 (*C*H$_2$CON), 29.2 (*C*H$_2$ Gln), 28.9 (*C*H$_2$ linker), 28.4 (*C*H$_2$ Asp), 26.7 (*C*H$_2$ Pro), 24.5 (*C*H$_2$ Pro), 25.3 (*C*H$_2$ linker), 29.1, 28.2, 27.4 (*C*H$_2$ linker).

MS-ESI (negative) *m/z*: 571.2 ([M]$^-$) (calculated 571.24).

HS-GlnProAsp

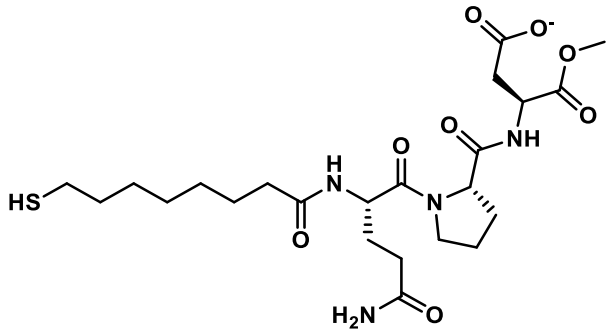

^{1}H NMR (500 MHz, MeOD + d$_7$-DMF): δ 4.76 – 4.66 (m, 1H, C*H* Asp), 4.56 – 4.44 (m, 1H, C*H* Pro), 4.39 – 4.33 (m, 1H, C*H* Gln), 3.90 – 3.70 (m, 2H, CH_2N Pro), 3.03 (s, 3H, OCH_3), 2.79 – 2.58 (m, 2H, CH_2 Gln), 2.46 (t, J = 7.7 Hz, 2H, CH_2CON), 2.33 (t, J = 7.2 Hz, 2H, CH_2SH), 2.29 – 2.20 (m, 2H, CH_2 Asp), 2.19 – 2.01 (m, 2H, CH_2 Pro), 2.01 – 1.90 (m, 2H, CH_2 Pro), 1.75 (m, 2H, CH_2CO Gln), 1.71 – 1.51 (m, 4H, 2 CH_2 linker), 1.46 – 1.24 (m, 6H, 3 CH_2 linker).

^{13}C NMR (126 MHz, MeOD + d_7-DMF): δ 174.37 (C=O), 171.62 (C=O), 169.02 (C=O), 163.47 (C=O), 163.23 (C=O), 163.00 (C=O), 60.2 (*C*H Gln), 52.7 (*C*H Pro), 50.5 (O*C*H_3 Asp), 50.1 (*C*H Asp), 47.9 (N*C*H_2 Pro), 39.2 (*C*H_2CON Gln), 30.9 (SH*C*H_2), 29.1 (*C*H_2CON), 35.6 (*C*H_2 Asp), 29.4 (*C*H_2 Gln), 27.9 (*C*H_2 Pro), 25.3 (*C*H_2 Pro), 24.9 (*C*H_2 linker), 25.3 (*C*H_2 linker), 29.5, 28.8, 27.0 (*C*H_2 linker).

HRMS (negative) *m/z*: 529.2309 ($[M]^-$) (calculated 529.2322).

AcS-TrpProAsp

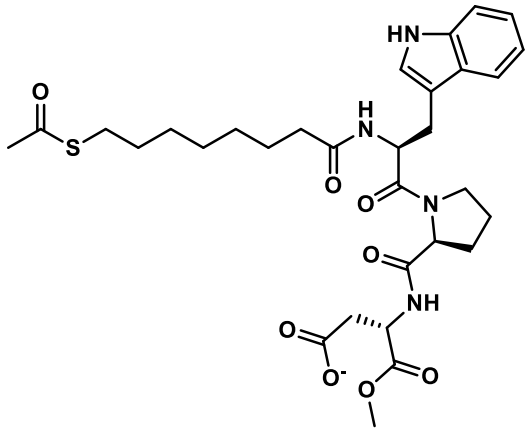

^{1}H NMR (500 MHz, MeOD): δ 8.19 – 8.12 (m, 1H, C*H* Trp), 7.65 (dd, J = 21.6, 7.6 Hz, 1H, C*H* Trp), 7.58 (s, 1H, C*H* Trp), 7.28 – 7.23 (m, 1H, C*H* Trp), 7.06 – 7.00 (m, 1H, C*H* Trp), 4.83 – 4.75 (m, 1H, C*H* Asp), 4.74 – 4.63 (m, 1H, C*H* Trp), 4.54 – 4.46 (m, 1H, C*H* Pro), 3.92 – 3.77 (m, 2H, NCH_2 Pro), 3.74 (s, 3H, OCH_3 Asp), 3.23 – 3.11 (m, 2H, CH_2 Trp), 2.85 – 2.79 (m, 4H, CH_2 Asp + CH_2SAc), 2.29 (s, 3H, CH_3COS), 2.26 – 1.87 (m, 6H, 2 CH_2 Pro + CH_2CON), 1.64 – 1.40 (m, 4H, 2 CH_2 linker), 1.39 – 1.02 (m, 6H, 3 CH_2 linker).

^{13}C NMR (126 MHz, MeOD): δ 196.33 (*C*OS), 174.59 (*C*=O), 174.34 (*C*=O), 172.67 (*C*=O), 172.43 (*C*=O), 171.98 (*C*=O), 136.62, 127.06, 109.44 (3C, quaternary *C* Trp), 124.4, 122.6, 119.0, 117.4, 114.7 (5C, *C*H Trp), 60.3 (*C*H Pro), 51.7 (OCH_3 Asp), 49.1 (*C*H Trp), 48.5 (*C*H Asp), 47.1 (NCH_2 Pro), 35.5 (*C*H_2 Asp), 35.4 (*C*H_2 Trp), 35.3 (*C*H_2SAc), 35.2 (*C*H_2CON), 29.1 (*C*H_3COS), 28.9, 24.5 (*C*H_2 Pro), 28.7 (*C*H_2 linker), 25.3 (*C*H_2 linker), 29.2, 28.9, 28.2 (*C*H_2 linker).

MS-ESI (negative) *m/z*: 629.2 ([M]$^{-}$) (calculated 629.27).

HS-TrpProAsp

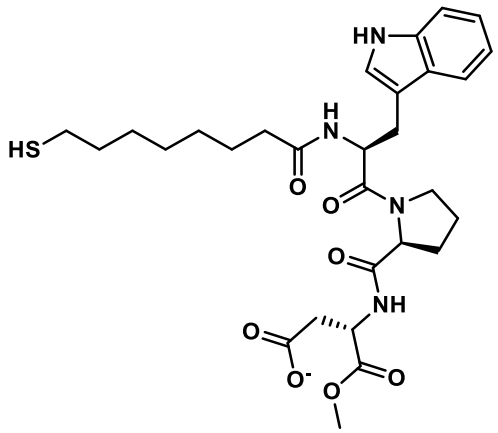

^{1}H NMR (500 MHz, MeOD): δ 7.65 (dd, J = 7.9, 5.3 Hz, 1H, C*H* Trp), 7.35 (dd, J = 8.2, 3.2 Hz, 1H, C*H* Trp), 7.22 (s, 1H, C*H* Trp), 7.09 (t, J = 7.4 Hz, 1H, C*H* Trp), 7.04 (t, J = 7.4 Hz, 1H, C*H* Trp), 5.05 – 4.98 (m, 1H, C*H* Asp), 4.53 – 4.47 (m, 1H, C*H* Pro), 4.47 – 4.42 (m, 1H, C*H* Trp), 3.76 –3.64 (m, 5H, NCH_2 Pro + CH_3O Asp), 3.20 – 3.08 (m, 2H, CH_2 Trp), 2.83 – 2.75 (m, 2H, CH_2 Asp), 2.72 – 2.61 (m, 2H, CH_2CON), 2.18 – 2.10 (m, 2H, CH_2SH), 2.13 – 1.89 (m, 4H, 2 CH_2 Pro), 1.70 – 1.54 (m, 2H, CH_2 linker), 1.53 – 1.43 (m, 2H, CH_2 linker), 1.41 – 1.13 (m, 6H, 3 CH_2 linker).

^{13}C NMR (126 MHz, MeOD): δ 175.7 (*C*=O), 173.9 (*C*=O), 172.9 (*C*=O), 172.5 (*C*=O), 171.2 (*C*=O), 136.9, 127.8, 109.1 (3C, quaternary *C* Trp), 123.7, 120.8, 118.4, 117.7, 110.8 (5C, *C*H Trp), 60.2 (*C*H Pro), 52.2 (*C*H Trp), 51.5 (*C*H Asp), 47.2 (N*C*H_2 Pro), 39.5 (*C*H_2 Asp), 39.2 (*C*H_2CON), 35.4 (HS*C*H_2), 28.7 (*C*H_2 linker), 28.6, 24.4 (2C, *C*H_2 Pro), 27.3 (*C*H_2 Trp), 24.9 (*C*H_2 linker), 29.1, 28.3, 28.1 (*C*H_2 linker).

HRMS (negative) *m/z:* 587.2489 ([M]$^-$) (calculated 587.2529).

AcS-ProLeuAsp

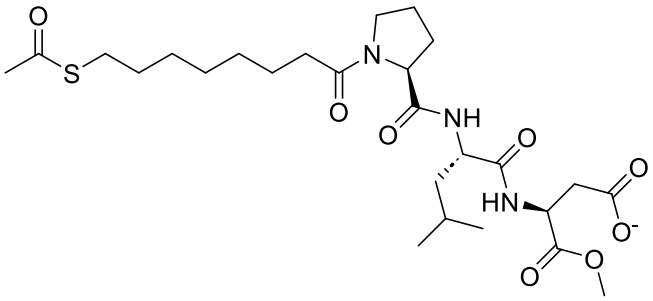

^{1}H NMR (500 MHz, MeOD, 25 °C): δ 4.77 (t, J = 5.8 Hz, 1H, C*H* Asp), 4.44 (m, 2H, C*H* Leu + C*H* Pro), 3.73 (s, 3H, CH_3O), 3.71 – 3.64 (m, 1H, 1/2 CH_2 Pro), 3.62 – 3.55 (m, 1H, 1/2 CH_2 Pro), 2.87 (m,, 4H, CH_2 Asp + CH_2S), 2.39 (t, 2H, CH_2CON), 2.31 (s, 3H, CH_3COS), 2.22 (m, 1H, 1/2 CH_2 Pro), 2.08 – 1.95 (m, 3H, 1/2 CH_2 Pro + CH_2 Pro), 1.81 – 1.70 (m, 1H, C*H* Leu), 1.69 – 1.55 (m, 6H, 1CH_2 Leu + 2 CH_2 linker), 1.43 – 1.29 (m, 6H, 3 CH_2 linker), 1.03 (d, J = 6.5 Hz, 3H, CH_3 Leu), 0.91 (d, J = 6.5 Hz, 3H, CH_3 Leu) .

^{13}C NMR (126 MHz, MeOD, 25 °C): δ 196.20 (*C*OS), 173.59 (*C*O), 173.42 (*C*O), 173.17 (*C*O), 172.43 (*C*O), 171.21 (*C*O), 59.98 (*C*H Pro), 51.68 (*C*H Leu), 51.59 (*C*H_3O), 48.86 (*C*H Asp), 47.40 (*C*H_2 Pro), 40.12 (*C*H_2 Leu), 35.32 (*C*H_2 Asp), 33.98 (*C*H_2CON), 29.36 (*C*H_2), 29.28 (CH_3S), 29.14, 28.81, 28.55 (*C*H_2 linker), 28.43 (*C*H_2S), 28.23 (*C*H_2 linker), 24.43 (*C*H Leu), 24.39, 24.31 (*C*H_2 linker), 22.09 (*C*H_3 Leu), 20.59 (*C*H_3 Leu).

HS-ProLeuAsp

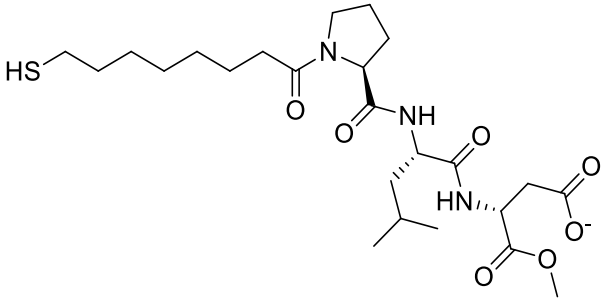

^{1}H NMR (500 MHz, MeOD): δ 4.75 (t, *J* = 5.8 Hz, 1H, C*H* Asp), 4.46 – 4.40 (m, 2H, C*H* Leu + C*H* Pro), 3.73 (s, 3H, CH_3O), 3.71 – 3.64 (m, 1H, ½ CH_2 Pro), 3.63 – 3.57 (m, 1H, ½ CH_2 Pro), 2.87 – 2.82 (m, 2H, CH_2 Asp), 2.51 (t, *J* = 7.2 Hz, 2H, CH_2SH), 2.40 (t, J = 5.7, 2H, CH_2CON), 2.27 – 2.17 (m, 1H, CH_2 Pro), 2.10 – 1.94 (m, 3H, CH_2 Pro), 1.77 (m, *J*, 1H, C*H* Leu), 1.67 – 1.56 (m, 6H, CH_2 Leu + 2 CH_2 linker), 1.48 – 1.30 (m, 6H, 3 CH_2 linker), 0.98 (d, *J* = 6.5 Hz, 3H, CH_3 Leu), 0.94 (d, *J* = 6.6 Hz, 3H, CH_3 Leu).

^{13}C NMR (126 MHz, MeOD) δ 173.57, 173.45, 173.18, 172.80, 171.32 (*C*=O), 60.24 (*C*H Pro), 59.94 (*C*H Leu), 51.70 (*C*H_3O), 51.56 (*C*H Asp), 48.93 (*C*H Asp), 47.38 (*C*H_2 Pro), 40.16 (*C*H_2 Leu), 35.58 (*C*H_2 Asp), 33.99 (*C*H_2CON), 33.75 (*C*H_2), 31.83 (*C*H_2 Pro), 29.11, 28.89, 28.56, 28.42, 28.22, 27.84, 24.42, 24.40, 23.54 (*C*H_2 linker), 22.08 (*C*H_3 iPr), 20.58 (*C*H_3 iPr).

HRMS (negative) m/z: 514.2588 (calculated 514.2592).

AcS-PheSerAsp

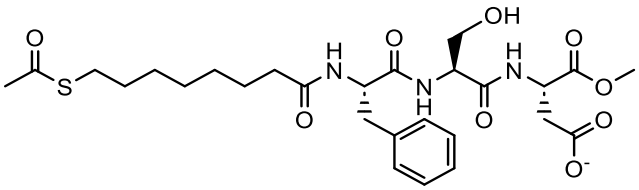

^{1}H NMR (500 MHz, MeOD, 25 °C): δ 7.34 – 7.17 (m, 5H, ArPhe), 4.80 (t, J = 5.3 Hz, 1H, C*H*, Asp), 4.71 (dd, J=10.1, 4.1 Hz, 1H, C*H* Phe), 4.47 (t, J=5.9 Hz, 1H, C*H* Ser), 3.82 (dd, J=11.3, 5.7 Hz, 2H, CH_2 Ser), 3.75 (s, 3H, CH_3O), 3.18 -2.84 (dd, J = 14.0, 4.7 Hz, 1H, CH_2 Phe), 2.91 (m, 4H, CH_2 Asp + CH_2S), 2.31 (s, 3H, CH_3COS), 2.16 (t, J = 8.2 Hz, 2H, CH_2CON), 1.54 (quint, J = 7.8 Hz, 2H, CH_2 linker), 1.48 (quint, J = 7.7 Hz, 2H, CH_2 linker), 1.37 - 1.11 (m, 6H, 3 CH_2 linker).

^{13}C NMR (126 MHz, MeOD, 25 °C) HSQC: δ 127.61, 125.7 (*C*H ArPhe), 61.04 (*C*H_2 Ser), 54.40 (*C*H Phe), 53.62 (*C*H Ser), 50.89 (*C*H_3O), 48.16 (*C*H Asp), 36.94 (*C*H_2 Asp), 36.84 (*C*H_2 Phe), 34.50 (*C*H_2CON), 28.65 (*C*H_2 linker), 28.26 (*C*H_3S), 27.48, 24.75 (*C*H_2 linker).

HS-PheSerAsp

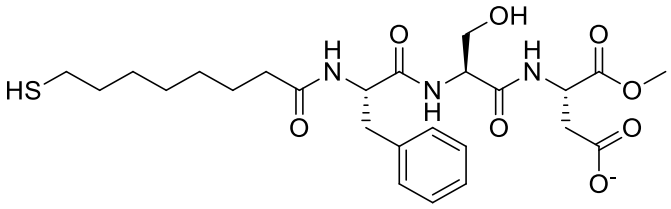

HRMS (negative) m/z: 538.2223 (calculated: 538.2228).

AcS-GlyIleAsp

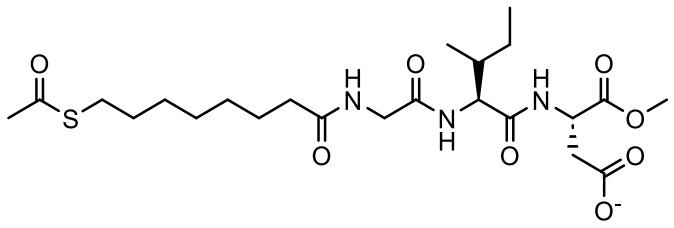

^{1}H NMR (500 MHz, MeOD): δ 4.78 (t, J = 6.0 Hz, 1H, C*H* Asp), 4.31 (d, J = 6.9 Hz, 1H, C*H* Ile), 3.92 (d, J = 16.6 Hz, 1H, C*H* Gly), 3.86 (d, J = 16.6 Hz, 1H, C*H* Gly), 3.72 (s, 3H, C*H*$_3$O), 2.89 (t, J= 7.3 Hz, 2H, CH$_2$S), 2.83 (d, J = 6.1 Hz, 2H, C*H*$_2$ Asp), 2.32 (s, 3H, C*H*$_3$COS), 2.28 (t, J = 7.6 Hz, 2H, C*H*$_2$CON), 1.88 (m, 1H, C*H* Ile), 1.64 (quint, J = 7.3 Hz, 2H, C*H*$_2$ linker), 1.57 (m, 2H, C*H*$_2$ linker), 1.53 (m, 1H, C*H*$_2$ Ile), 1.19 (m, 1H, C*H*$_2$ Ile), 1.37 (m, 6H, 3 C*H*$_2$ linker), 0.98 (d, J = 6.9 Hz, 3H, CHC*H*$_3$ Ile), 0.93 (t, J = 7.5 Hz, 3H, CH$_2$C*H*$_3$ Ile)

^{13}C NMR (500 MHz, MeOD) HSQC: δ 57.47 (α*C*H Ile), 51.61 (*C*H$_3$O), 48.88 (*C*H Asp), 42.25 (*C*H Gly), 35.61 (*C*H$_2$ Asp), 35.22 (*C*H$_2$CON), 31.17 (*C*H Ile), 29.37, 25.05 (*C*H$_2$ linker), 28.98 (*C*H$_3$COS), 28.59 (*C*H$_2$ linker), 28.20 (*C*H$_2$S), 24.30 (*C*H$_2$ Ile), 14.15 (CH*C*H$_3$, Ile), 10.64 (CH$_2$*C*H$_3$ Ile).

HS-GlyIleAsp

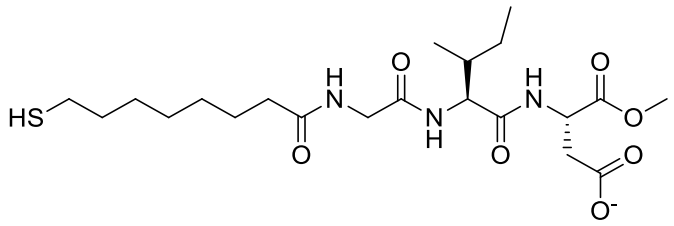

HRMS (negative) m/z: 474.2275 (calculated:474.2279).

AcS-ProProAsp

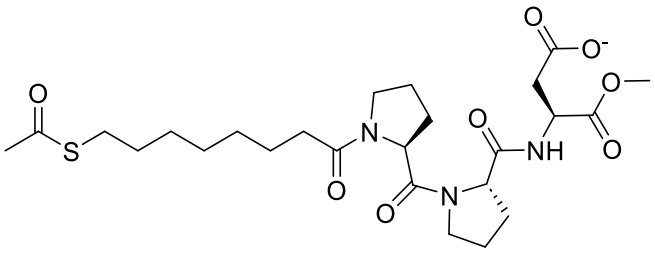

^{1}H NMR (500 MHz, MeOD): δ 4.74 (t, J = 5.8 Hz, 1H, C*H* Asp), 4.67 (m, 1H, C*H* Pro), 4.51 (m, 1H, C*H* Pro), 3.73 (s, 3H, CH_3O), 3.70 – 3.54 (m, 4H, CH_2N Pro), 2.88 (t, J = 6.9 Hz, 2H, CH_2S), 2.79 (dd, J = 7.2, 5.5 Hz, 1H, CH_2 Asp), 2.87 (dd, J = 7.2, 5.5 Hz, 1H, CH_2 Asp), 2.37 (t, J = 6.9 Hz, 2H, CH_2CON), 2.32 (s, 3H, CH_3COS), 2.30 – 1.84 (m, 8H, CH_2 Pro), 1.65 – 1.54 (m, 4H, 2 CH_2 linker), 1.44 – 1.30 (m, 6H, 3 CH_2 linker).

^{13}C NMR (500 MHz, MeOD) HSQC: δ 59.81 (*C*H Pro), 57.86 (*C*H Pro), 51.61 (*C*H_3O), 48.88 (*C*H Asp), 46.93 47.32 (*C*H_2N Pro), 36.00 35.61 (*C*H_2 Asp), 34.05 (*C*H_2CON), 29.37, 24.30 (*C*H_2 linker), 28.98 (*C*H_3COS), 28.59 (*C*H_2 linker), 28.58, 24.69 (*C*H_2 Pro), 28.20 (*C*H_2S).

HS-ProProAsp

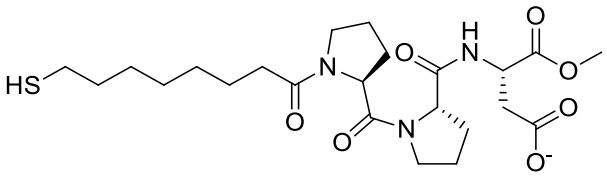

HRMS (negative) m/z: 498.2276 (calculated:498.2279).

AcS-PheLeuAsp

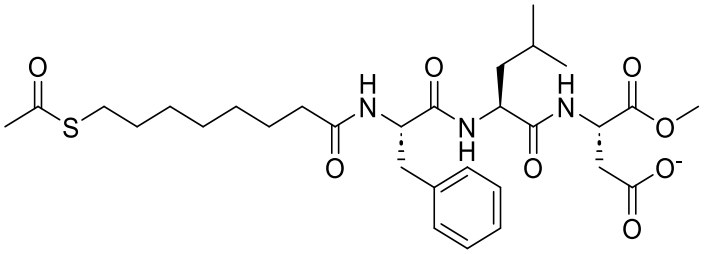

^{1}H NMR (500 MHz, MeOD): δ 7.31 – 7.17 (m, 5H, Ph Phe), 4.82 – 4.74 (m, 2H, C*H* Asp + C*H* Phe), 4.51 (dd, J = 9.2, 5.6 Hz, 1H, C*H* Leu), 3.72 (s, 3H, OCH_3), 3.18 (dd, J = 14.0, 4.7 Hz, 2H, CH_2Phe), 2.93 – 2.81 (m, 4H, CH_2 Asp + CH_2S), 2.31 (s, 3H, CH_3S), 2.15 (t, J = 7.4 Hz, 2H, CH_2CON), 1.75 – 1.57 (m, 3H, C*H* Leu + CH_2 Leu), 1.56 – 1.42 (m, 4H, 2 CH_2 linker), 1.36 – 1.09 (m, 6H, 3 CH_2 linker), 0.94 (d, J = 6.4 Hz, 6H, CH_3 Leu).

^{13}C NMR (126 MHz, MeOD): δ 196.28 (*C*OS), 174.70 (*C*O linker), 173.00 (*C*=O), 172.52 (*C*=O), 172.41 (*C*=O), 171.23 (*C*=O), 137.24 (C quat. Ph), 129.03 (Ph), 128.07 (Ph), 126.39 (Ph), 54.30 (*C*H Phe), 51.75 (*C*H_3O), 51.66 (*C*H Leu), 48.83 (*C*H Asp), 40.65 (*C*H_2 Leu), 37.51 (*C*H_2 Phe), 35.44 (*C*H_2CON), 35.36 (*C*H_2 Asp), 29.31 (*C*H_3COS), 28.52 (*C*H_2SAc + *C*H_2 linker), 28.33, 28.24), 25.44 (*C*H_2 linker), 24.39 (*C*H Leu), 23.37 (*C*H_2 linker), 22.14 (*C*H_3 Leu), 20.91 (*C*H_3 Leu).

HS-PheLeuAsp

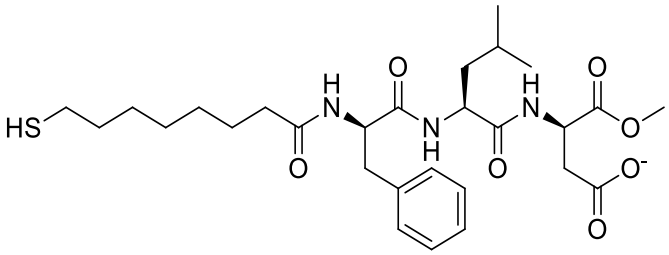

^{1}H NMR (500 MHz, MeOD): δ 7.32 – 7.17 (m, 5H, Ar Phe), 4.76 – 4.66 (m, 2H, C*H* Phe + C*H* Asp), 4.50 – 4.37 (m, 1H, C*H* Leu), 3.72 (s, 3H, CH_3O), 3.28 – 3.19 (m, 1H, CH_2 Phe), 2.93 – 2.85 (m, 1H, CH_2 Phe), 2.80 – 2.58 (m, 2H, CH_2 Asp), 2.48 (t, J = 7.1 Hz, 2H, CH_2S), 2.15 (t, J = 7.4 Hz, 2H, CH_2CON), 1.86 – 1.53 (m, 3H, C*H* Leu + CH_2 Leu), 1.51 – 1.41 (m, 4H, 2 CH_2 linker), 1.40 – 1.30 (m, 2H, CH_2 linker), 1.29 – 1.22 (m, 2H, CH_2 linker), 1.19 – 1.11 (m, 2H, CH_2 linker), 0.98 (d, J = 6.3 Hz, 3H, CH_3 Leu), 0.94 (d, J = 6.7 Hz, 3H, CH_3 Leu).

^{13}C NMR (126 MHz, MeOD): δ 176.48 (*C*=O), 174.75 (*C*=O), 172.75 (*C*=O), 172.53 (*C*=O), 171.89 (*C*=O), 169.09 (*C*=O), 137.46 (*C* quat Phe), 128.96 (*C*H Phe), 128.00 (*C*H Phe), 126.28 (*C* quat Phe), 54.33 (*C*H Phe), 51.88 (*C*H Leu), 49.93 (*C*H Asp), 48.46 (*C*H_3O), 39.99 (*C*H_2 Leu), 38.37 (*C*H_2 Asp),

37.18 (*C*H_2 Phe), 35.56 (*C*H_2CON), 31.08, 30.26, 28.77, 27.88, 25.52 (*C*H_2 linker), 24.33 (*C*H Leu), 22.13 (*C*H_3 Leu), 20.67 (*C*H_3 Leu).

HRMS (negative) m/z: 564.2746 (calculated: 564.2749).

AcS-LeuLeuAsp

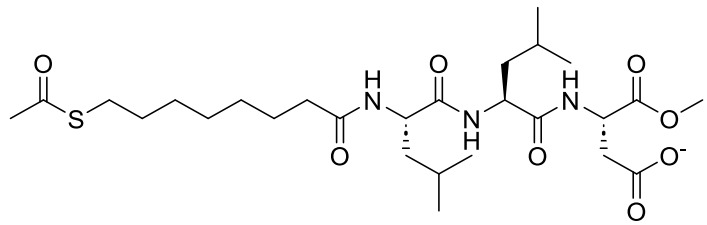

^{1}H NMR (500 MHz, MeOD): δ 4.77 (dd, *J* = 5.7 Hz, 1H, CH Asp), 4.48 (m, 2H, 2 C*H* Leu), 3.73 (s, 3H, CH_3O), 2.91 – 2.80 (m, 4H, CH_2SAc + CH_2 Asp), 2.31 (s, 3H, CH_3S), 2.25 (t, *J* = 7.3 Hz, 2H, CH_2COON), 1.76 – 1.53 (m, 10H, 2 CH_2 linker + 2 C*H* Leu + 2 CH_2 Leu), 1.42 – 1.30 (m, 6H, 3 CH_2 linker), 0.95 (4d, *J* = 6.1 Hz, 12H, CH_3 Leu).

^{13}C NMR (126 MHz, MeOD): δ 196.19 (*C*OS), 174.84 (*C*=O), 173.48 (*C*=O), 173.00 (*C*=O), 172.38 (*C*=O), 171.19 (*C*=O), 51.67 (O*C*H$_3$), 51.61 (*C*H Leu), 48.79 (*C*H Asp), 40.58 (*C*H$_2$ Leu), 35.42 (*C*H$_2$ Asp), 35.39 (*C*H$_2$CON), 29.30 (*C*H$_3$S), 29.26, 28.69 (*C*H$_2$ linker), 28.50 (*C*H$_2$Sac + *C*H$_2$ linker), 28.29, 25.52 (*C*H$_2$ linker), 24.56 (*C*H Leu), 24.39 (*C*H Leu), 22.15 (*C*H$_3$ Leu), 20.83 (*C*H$_3$ Leu), 20.70 (*C*H$_3$ Leu).

HS-LeuLeuAsp

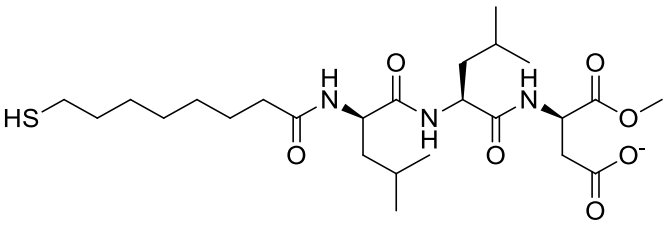

^{1}H NMR (500 MHz, MeOD): δ 4.70 – 4.65 (m, 1H, C*H* Asp), 4.49 – 4.42 (m, 2H, C*H* Leu), 3.72 (s, 3H, CH_3O), 2.75 (dd, J = 16.2, 5.7 Hz, 1H, CH_2 Asp), 2.60 (dd, J = 16.2, 5.0 Hz, 1H, CH_2 Asp), 2.51 (t, *J* = 7.1 Hz, 2H, CH_2S), 2.26 (t, J = 7.5 Hz, 2H, CH_2CON), 1.81 – 1.53 (m, 10H, 2 CH_2 linker + 2 C*H* Leu + 2 CH_2 Leu), 1.47 – 1.29 (m, 6H, 3 CH_2 linker), 1.02 – 0.90 (m, 12H, CH_3 Leu).

^{13}C NMR (126 MHz, MeOD): δ 176.33 (C=O), 174.96 (C=O), 173.53 (*C*=O), 172.84 (*C*=O), 172.39 (*C*=O), 51.66 (*C*H Leu), 49.92 (*C*H Asp), 40.59 (*C*H$_2$ Leu), 40.20 (*C*H$_2$ Leu), 38.51 (*C*H$_2$ Asp), 35.42 (*C*H$_2$CON), 33.73, 28.75, 28.49, 27.87, 24.57 (*C*H$_2$ linker), 24.57 (*C*H Leu), 24.38 (*C*H Leu), 22.14 (*C*H$_3$ Leu), 22.12 (*C*H$_3$ Leu), 20.59 (*C*H$_3$ Leu), 20.47 (*C*H$_3$ Leu).

HRMS (negative) m/z: 530.2935 (calculated: 530.2905).

AcS-Trp(Boc)GlnAsp

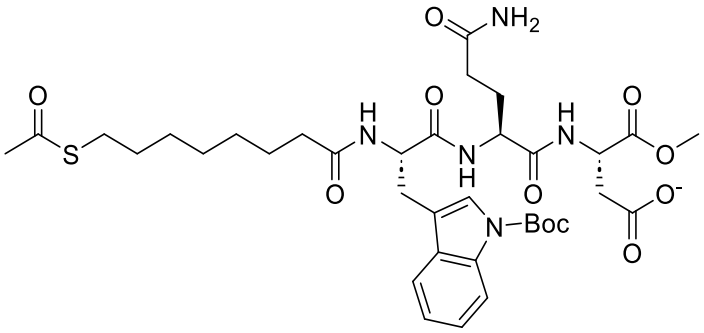

^{1}H NMR (500 MHz, MeOD): δ 8.09 (d, J = 8.1 Hz, 1H, C*H* Trp), 7.65 (t, J = 8.1 Hz, 1H, C*H* Trp), 7.54 (s, 1H, C*H* Trp), 7.30 (t, J = 7.8 Hz, 1H, C*H* Trp), 7.23 (t, J = 7.5 Hz, 1H, C*H* Trp), 4.81 – 4.74 (m, 2H, C*H* Asp + C*H* Trp), 4.46 (dd, J = 8.6, 5.2 Hz, 1H, C*H* Gln), 3.73 (s, 3H, CH_3O), 3.25 (m, 1H, ½ CH_2 Trp), 3.06 (m, 1H, ½ CH_2 Trp), 2.87 (t, J = 7.4 Hz, 2H, CH_2 Asp), 2.80 (t, J = 7.4 Hz, 2H, CH_2S), 2.34 (t, J = 7.8 Hz, 2H, CH_2CON), 2.30 (s, 3H, CH_3S), 2.22 – 2.07 (m, 3H, CH_2 Gln + ½ CH_2 Gln), 2.03 – 1.89 (m, 1H, ½ CH_2 Gln), 1.68 (s, 9H, CH_3 Boc), 1.52 – 1.41 (m, 4H, 2 CH_2 linker), 1.27 – 1.05 (m, 6H, 3 CH_2 linker).

^{13}C NMR (126 MHz, MeOD): δ 196.26 (*C*OS), 176.47 (*C*O), 175.02 (*C*O), 172.50 (*C*O), 172.43 (*C*O), 171.88 (*C*O), 171.30 (*C*O), 149.63 (*C*O Boc), 135.37 (quaternary *C* Boc), 130.38 (quaternary *C* Boc), 124.09 (*C*H Boc), 123.95 (*C*H Boc), 122.29 (*C*H Boc), 118.84 (*C*H Boc), 116.14 (quaternary *C* Boc), 114.78 (*C*H Boc), 83.43 (1C., quaternary *C* Boc), 53.11 (*C*H Trp), 52.61 (*C*H Gln), 51.70 (*C*H_3O), 48.86 (*C*H Asp), 35.45 (*C*H_2 Trp), 35.35 (*C*H_2 Asp), 30.91 (*C*H_2CON), 29.24 (*C*H_2 linker), 29.17 (*C*H_3S), 28.47, 28.43, 28.40 (*C*H_2 linker), 28.14 (*C*H_2S), 27.65 (*C*H_2 Gln), 27.12 (*C*H_3 Boc), 26.92 (*C*H_2 Asp), 25.30 (*C*H_2 linker).

HS-TrpGlnAsp

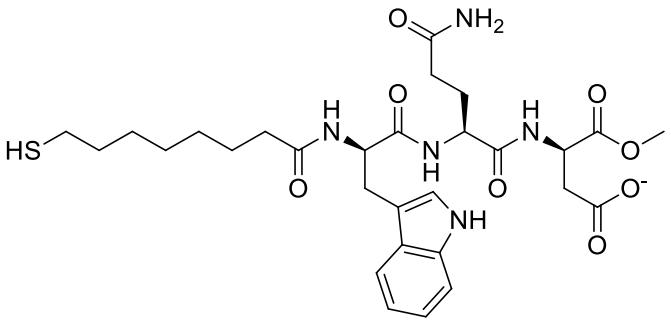

^{1}H NMR (500 MHz, MeOD): δ 8.15 (d, *J* = 8.3 Hz, 1H, C*H* Trp), 7.62 (d, *J* = 7.7 Hz, 1H, C*H* Trp), 7.35 (d, *J* = 8.2 Hz, 1H, C*H* Trp), 7.10 (t, *J* = 7.5 Hz, 1H, C*H* Trp), 7.03 (t, *J* = 7.5 Hz, 1H, C*H* Trp),

4.75 (t, *J* = 6.0 Hz, 1H, C*H* Asp), 4.67 (dd, *J* = 8.6, 5.4 Hz, 1H, C*H* Trp), 4.39 (dd, *J* = 8.7, 5.0 Hz, 1H, C*H* Gln), 3.74 (s, 3H, C*H*$_3$O Asp), 3.34 – 3.27 (m, 1H, 1/2 C*H*$_2$ Trp), 3.14 (dd, *J* = 14.8, 8.6 Hz, 1H, ½ C*H*$_2$ Trp), 2.97 – 2.77 (m, 4H, C*H*$_2$ Asp + C*H*$_2$ Gln), 2.38 – 2.24 (m, 2H, C*H*$_2$S), 2.18 (t, *J* = 7.0 Hz, 2H, C*H*$_2$CON), 2.10 (dtd, *J* = 15.7, 7.9, 7.5, 3.7 Hz, 1H, 1/2 C*H*$_2$ Gln), 1.99 – 1.85 (m, 1H, 1/2 C*H*$_2$ Gln), 1.50 (m, 4H, 2 C*H*$_2$ linker), 1.41 – 1.07 (m, 6H, 3 C*H*$_2$ linker).

^{13}C NMR (126 MHz, D_2O): δ 178.77, 178.21, 177.80, 175.64, 173.22, 171.77 (*C*=O), 136.13 (C_{quat} Trp), 127.28 (C_{quat} Trp), 124.23 (*C*H Trp), 121.60 (*C*H Trp), 119.10 (*C*H Trp), 118.18 (*C*H Trp), (CH Trp), 109.01 (C_{quat} Trp), 54.41 (*C*H Asp), 53.18 (*C*H Gln), 52.76 (*C*H Trp), 48.86 (*C*H$_3$O), 38.93 (*C*H$_2$CON), 35.76 (*C*H$_2$ Asp), 30.94 (*C*H$_2$S), 28.76, 28.46, 28.13, 27.51 (*C*H$_2$ Trp), 27.29, 25.29 (*C*H$_2$ linker).

HRMS (negative) m/z: 618.2599 (calculated: 618.2603).

AcS-ProAlaAsp

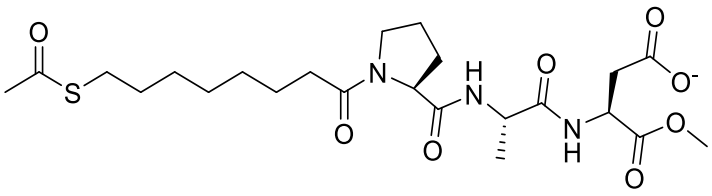

^{1}H NMR (500 MHz, MeOD): δ 4.76 (t, J = 5.5 Hz, 1H, CH Asp), 4.44 – 4.38 (m, 2H, C*H* Ala + C*H* Pro), 3.73 (s, 3H, CH_3O), 3.71 – 3.55 (m, 2H, CH_2 Asp), 2.87 (t, 2*H*, CH_2S), 2.40 (m, 2H, CH_2CON), 2.32 (s, 3H, CH_3S), 2.23 (m, 1H, ½ CH_2 Pro), 2.02 (m, , 3H, CH_2 Pro + ½ CH_2 Pro), 1.66 – 1.54 (m, 4H, 2 CH_2 linker), 1.44 – 1.30 (m, 9H, CH_3 Ala + 3 CH_2 linker).

^{13}C NMR (126 MHz, MeOD): δ 196.19 (*C*OS), 173.49 (*C*=O), 173.44 (*C*=O), 173.31 (*C*=O), 172.52 (*C*=O), 171.26 (*C*=O), 59.88 (*C*H Ala), 51.68 (*C*H_3O), 48.85 (*C*H Pro), 48.73 (*C*H Asp), 47.40 (*C*H_2 Pro), 35.30 (*C*H2 Asp), 33.93 (*C*H_2CON), 29.50 (*C*H_2 Pro), 29.38 (*C*H_2 linker), 29.20 (*C*H_2 Pro), 28.86, 28.65, 28.29, 24.40 (*C*H_2 linker), 24.28 (*C*H_2 Pro), 16.29 (*C*H_3 Ala).

HS-ProAlaAsp

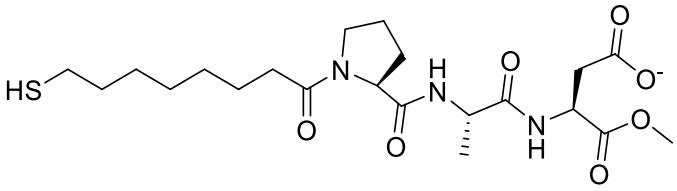

^{1}H NMR (500 MHz, MeOD): δ 4.73 – 4.63 (m, 1H, C*H* Asp), 4.46 – 4.38 (m, 2H, C*H* Ala + Pro), 3.72 (s, 3H, CH_3O), 3.68 (m, 1H, CH_2 Pro), 3.59 (m, 1H, CH_2 Pro), 2.79 (dd, *J* = 16.3, 5.7 Hz, 1H, CH_2 Asp), 2.63 (dd, *J* = 16.3, 5.0 Hz, 1H, CH_2 Asp), 2.51 (t, *J* = 7.1 Hz, 2H, CH_2S), 2.40 (t, *J* = 7.7 Hz, 2H,, CH_2CON), 2.28 – 2.19 (m, 2H, CH_2 Pro), 2.14 – 2.06 (m, 2H, CH_2 Pro + CH_2 Pro), 2.03 – 1.94 (m, 1H, CH_2 Pro), 1.67 – 1.54 (m, 4H, 2 CH_2 linker), 1.40 (d, *J* = 7.2 Hz, 3H, CH_3 Ala), 1.43 – 1.33 (m, 6H, 3 CH_2 linker).

^{13}C NMR (126 MHz, MeOD): δ 175.90 (*C*O), 175.60 (*C*O), 173.43 (*C*O), 173.23, (*C*O) 172.32 (*C*O), 59.93 (*C*H Ala), 51.40 (*C*H_3O), 49.71 (*C*H Asp), 48.99 (*C*H Pro), 47.44 (*C*H_2 Pro), 38.16 (*C*H_2 Asp), 33.94 (*C*H_2CON), 29.47 (*C*H_2 Pro), 29.28, 28.81, 28.55, 28.42, 28.22 (*C*H_2 linker), 24.40 (*C*H_2 Pro), 24.29 (*C*H_2 linker), 16.46 (*C*H_3 Ala).

HRMS (negative) m/z: 472.2118 (calculated: 472.2123).

HS-GlnGlnAsp

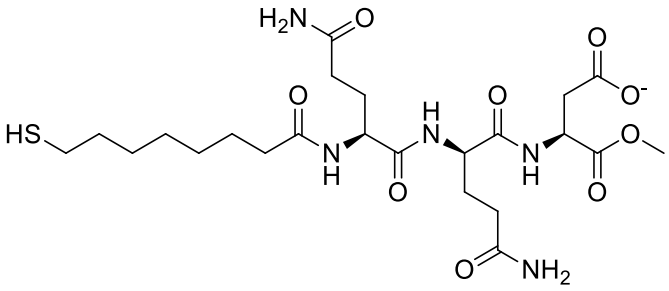

^{1}H NMR (500 MHz, MeOD): δ 4.74 – 4.66 (m, 1H, C*H* Asp), 4.44 (m, 1H, C*H* Gln), 4.35 – 4.28 (m, 1H, C*H* Gln), 3.72 (s, 3H, CH_3O), 2.84 – 2.75 (m, 1H, CH_2 Asp), 2.60 (dd, *J* = 20.1, 4.1 Hz, 1H, CH_2 Asp), 2.51 (t, *J* = 7.2 Hz, 2H, CH_2SH), 2.37 (t, *J* = 7.5 Hz, 2H, CH_2CON), 2.26 (t, *J* = 7.6 Hz, 4H, CH_2 Gln), 2.15 – 1.90 (m, 4H, CH_2 Gln), 1.72 – 1.55 (m, 4H, 2 CH_2 linker), 1.47 – 1.33 (m, 6H, 3 CH_2 linker).

^{13}C NMR (126 MHz, MeOD): δ 176.44 (*C*O), 176.40 (*C*O), 176.32 (*C*O), 174.99 (*C*O), 172.66 (*C*O), 172.51 (*C*O), 171.86 (*C*O), 53.12 (*C*H Gln), 52.75 (*C*H Gln), 51.42 (*C*H$_3$O), 49.91 (*C*H Asp), 38.42 (*C*H$_2$ Asp), 35.34 (*C*H$_2$ Gly),31.05 (*C*H$_2$CON), 30.25 (*C*H$_2$SH), 28.81, 28.49, 27.90 (*C*H$_2$ linker), 27.64 (*C*H$_2$ Gln), 27.16, 25.36 (*C*H$_2$ linker).

HRMS (negative) m/z: 560.2404 (calculated: 560.2396).

AcS-GlnAlaAsp

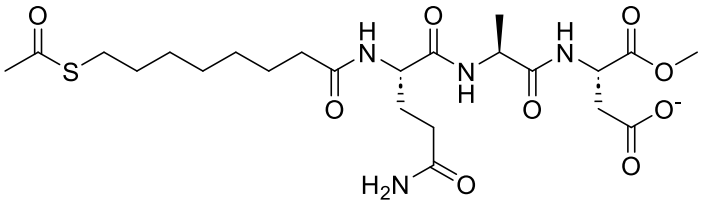

^{1}H NMR (500 MHz, MeOD): δ 4.78 (t, J = 5.8 Hz, 1H, C*H* Asp), 4.41 (q, J = 7.1 Hz, 1H, C*H* Gln), 4.38 – 4.29 (m, 1H, C*H* Ala), 3.74 (s, 3H, CH_3O), 2.91 – 2.83 (m, 4H, CH_2S + CH_2 Asp), 2.37 – 2.30 (m, 5H, CH_3S + CH_2CON linker), 2.26 (t, J = 7.5 Hz, 2H, CH_2 Gln), 2.13 – 1.91 (m, 2H, CH_2 Gln), 1.68 – 1.54 (m, 4H, 2 CH_2 linker), 1.39 (d, J = 7.2 Hz, 3H, CH_3 Ala), 1.43 – 1.30 (m, 6H, 3 CH_2 linker).

^{13}C NMR (126 MHz, MeOD): δ 196.28 (*C*OS), 176.47 (*C*=O), 174.92 (*C*=O), 173.34 (*C*=O), 172.55 (*C*=O), 172.17 (*C*=O), 171.32 (*C*=O), 52.69 (*C*H Ala), 51.63 (*C*H_3O), 48.87 (*C*H Asp + *C*H Gln), 35.40 (*C*H_2 Asp), 35.35 (*C*H_2 Asp), 35.40 *C*H_2 Gln), 31.09 (*C*H_2CON), 29.28, 29.13, 28.70 (*C*H_2 linker), 28.43 (*C*H_2S), 28.21 (*C*H_2 linker), 27.49 (*C*H_2 Gln), 25.32 (*C*H_2 linker), 16.57 (*C*H_3 Ala).

HS-GlnAlaAsp

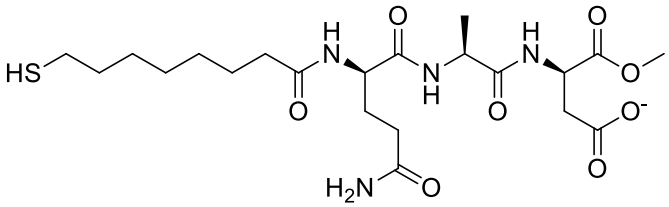

^{1}H NMR (500 MHz, MeOD): δ 4.82 – 4.77 (m, 1H, C*H* Asp), 4.54 – 4.49 (m, 1H, C*H* Gln), 4.49 – 4.43 (m, 1H, C*H* Ala), 3.75 (s, 3H, CH_3O), 2.98 (t, 2H, J = 7.3 Hz, CH_2S), 2.93 – 2.62 (m, 2H, CH_2 Asp), 2.47 – 2.40 (m, 2H, CH_2CON), 2.35 (t, J = 7.5 Hz, 2H, CH_2 Gln), 1.75 – 1.62 (m, 2H, CH_2 Gln), 1.73 (m, 2H, CH_2 linker), 1.67 (m, 2H, CH_2 linker), 1.49 (d, J = 7.2 Hz, 3H, CH_3 Ala), 1.47 – 1.39 (m, 6H, 3 CH_2 linker).

^{13}C NMR (126 MHz, MeOD): δ 176.45 (*C*=O), 176.03 (*C*=O), 174.85 (*C*=O), 173.17 (*C*=O), 172.47 (*C*=O), 172.27 (*C*=O),52.75 (*C*H Ala), 49.75 (*C*H Asp), 49.07 (*C*H Gln), 48.48 (*C*H_3O), 38.17 (*C*H_2 Asp), 35.37 (*C*H_2 Gln), 31.07 (*C*H_2CON), 29.28 (*C*H_2 linker), 28.46 (*C*H_2S), 28.43, 28.22 (*C*H_2 linker), 27.47 (*C*H_2 Gln), 25.34 (*C*H_2 linker), 16.59 (*C*H_3 Ala).

HRMS (negative) m/z: 503.2187 (calculated: 503.2181).

Characterization of TrpPheAsp-AuNP

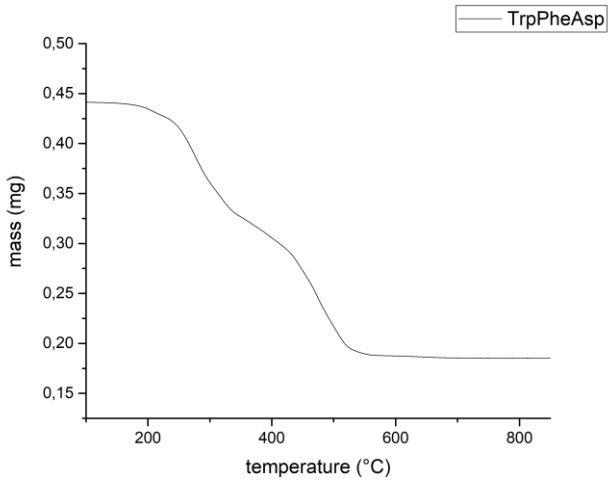

Figure S3. TGA analysis of TrpPheAsp-AuNP, weight loss = 58.10 %.

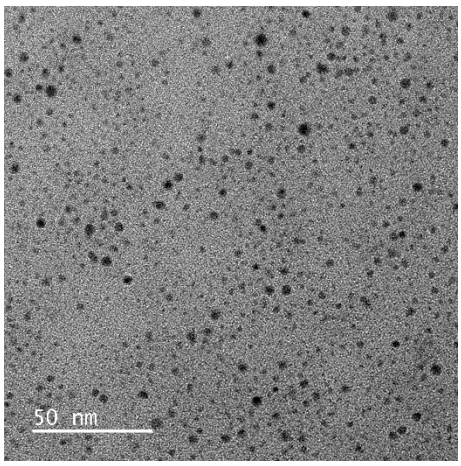

Figure S4. TEM analysis of TrpPheAsp-AuNP.

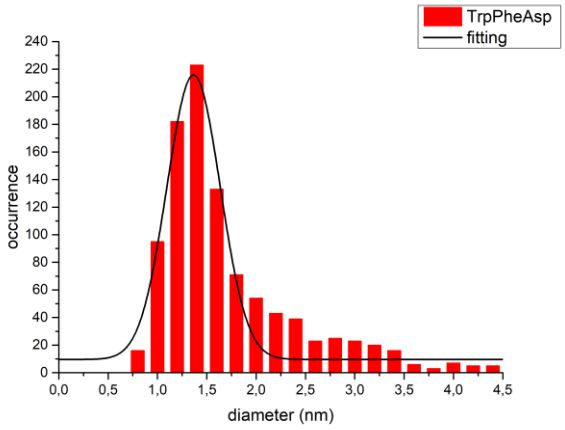

Figure S5. Sizing of TrpPheAsp-AuNP**,** average diameter = 1.4 ± 0.3 nm, average cluster formula: $Au_{80}SR_{34}$.

Characterization of TyrProAsp-AuNP

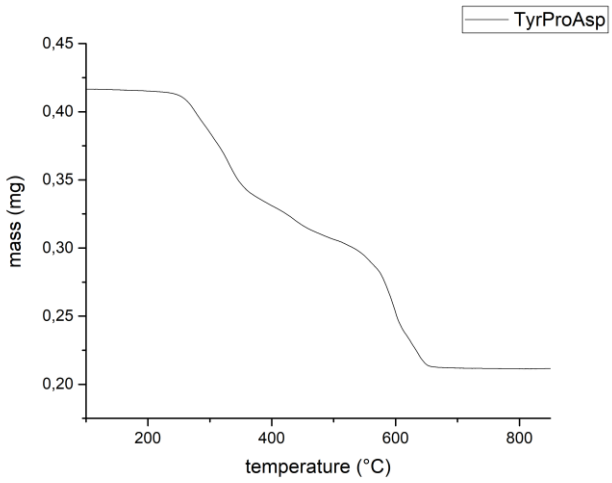

Figure S6. TGA analysis of TyrProAsp-AuNP, weight loss = 49.10 %.

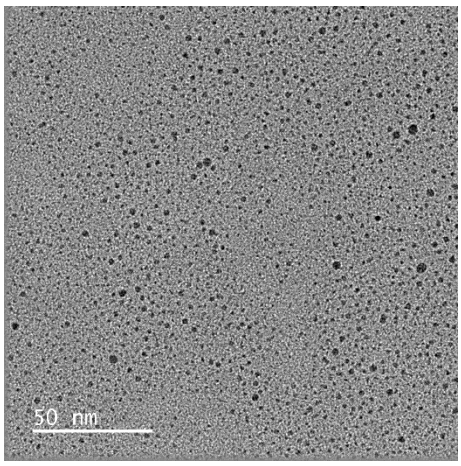

Figure S7. TEM analysis of TyrProAsp-AuNP.

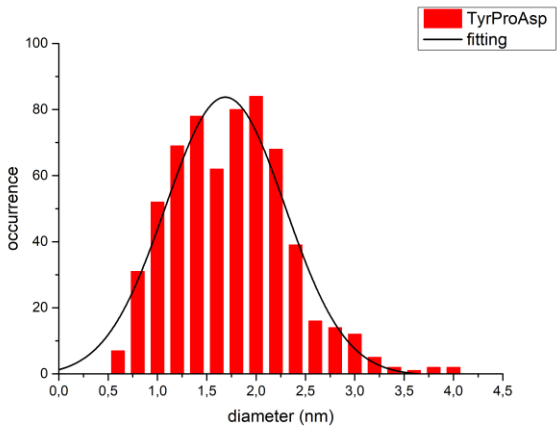

Figure S8. Sizing of TyrProAsp-AuNP**,** average diameter = 1.7 ± 0.6 nm, average cluster formula: $Au_{147}SR_{49}$.

Characterization of GlnProAsp-AuNP

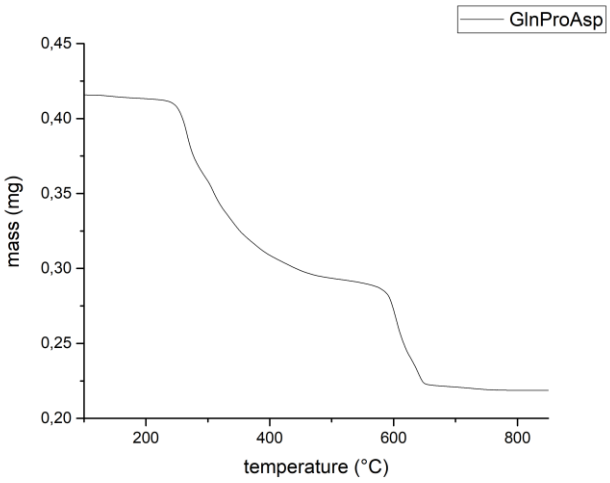

Figure S9. TGA analysis of GlnProAsp-AuNP, weight loss = 46.85 %.

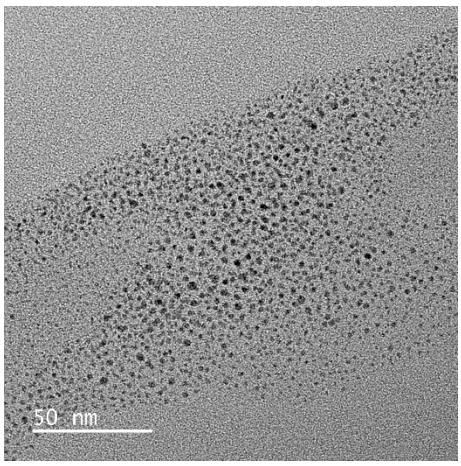

Figure S10. TEM analysis of GlnProAsp-AuNP.

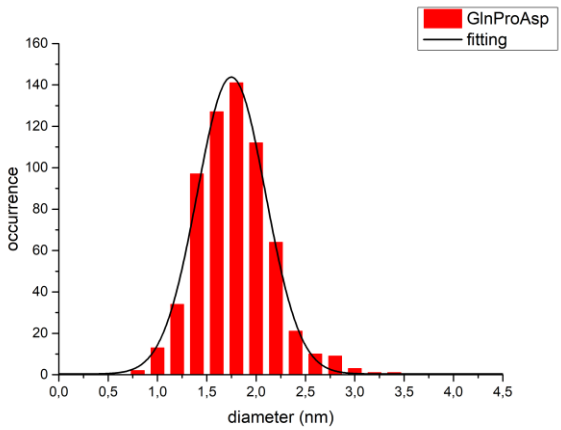

Figure S11. Sizing of GlnProAsp-AuNP**,** average diameter = 1.8 ± 0.3 nm, average cluster formula: $Au_{165}SR_{49}$.

Characterization of TrpProAsp-AuNP

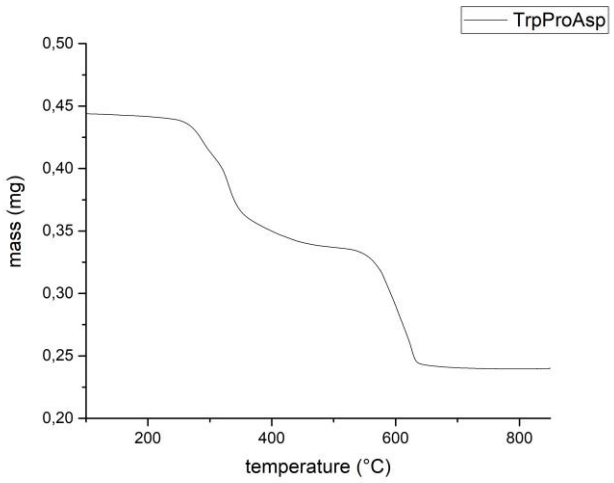

Figure S12. TGA analysis of TrpProAsp-AuNP, weight loss = 45.84 %.

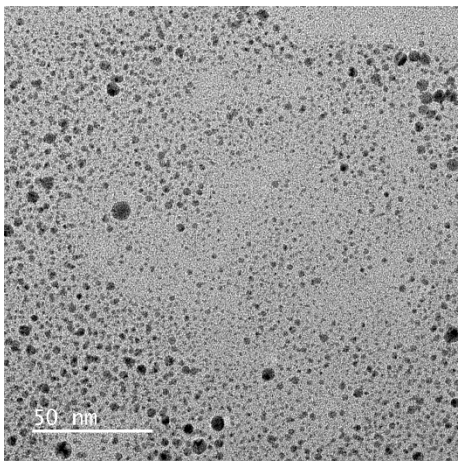

Figure S13. TEM analysis of TrpProAsp-AuNP.

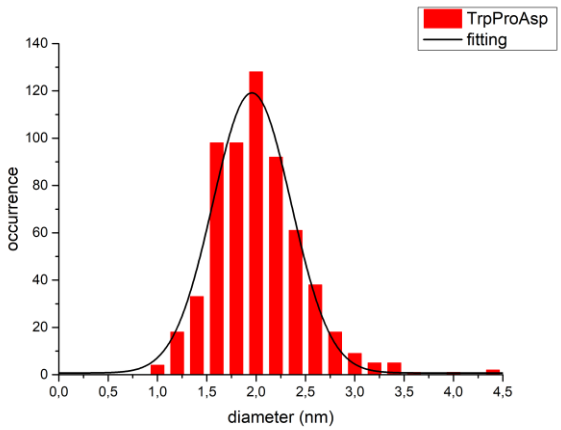

Figure S14. Sizing of TrpProAsp-AuNP**,** average diameter = 2.0 ± 0.4 nm, average cluster formula: $Au_{232}SR_{66}$.

Characterization of ProLeuAsp-AuNP

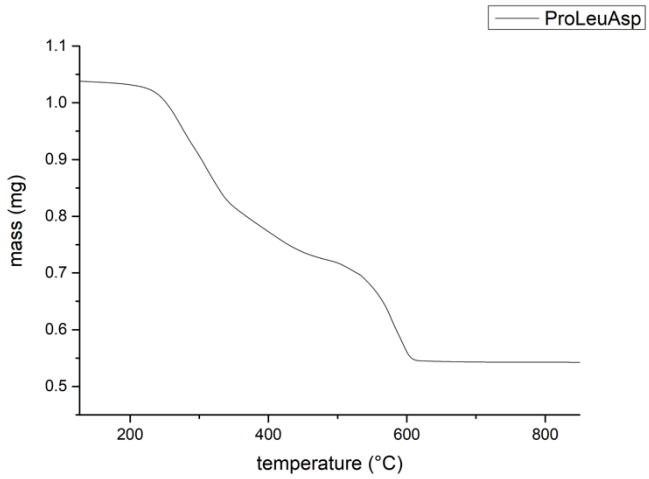

Figure S15. TGA analysis of ProLeuAsp-AuNP, weight loss = 47.73 %.

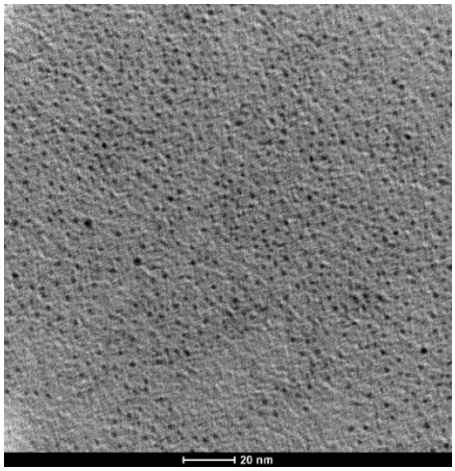

Figure S16. TEM analysis of ProLeuAsp-AuNP.

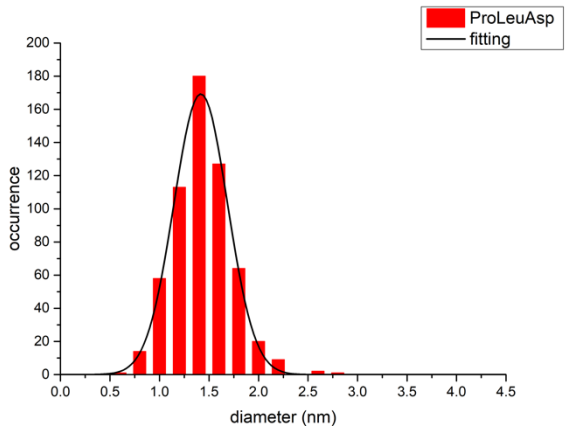

Figure S17. Sizing of ProLeuAsp-AuNP**,** average diameter = 1.4 ± 0.3 nm, average cluster formula: $Au_{88}SR_{31}$.

Characterization of PheSerAsp-AuNP

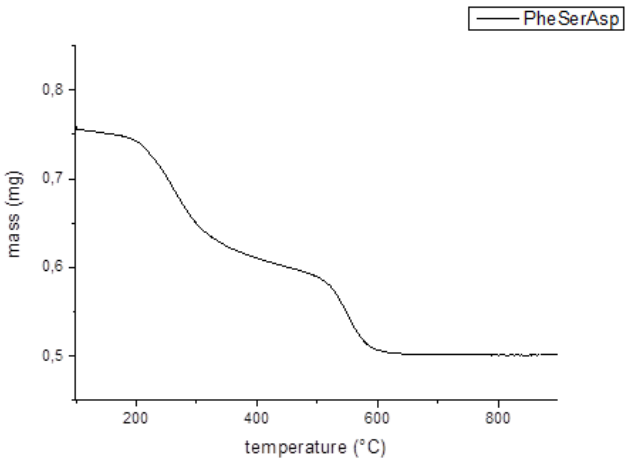

Figure S18. TGA analysis of PheSerAsp-AuNP, weight loss = 32.07 %.

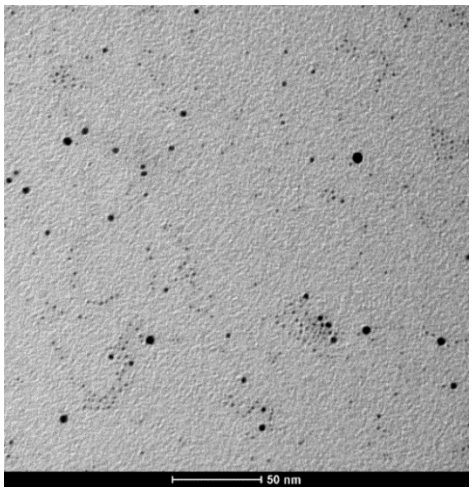

Figure S19. TEM analysis of PheSerAsp-AuNP.

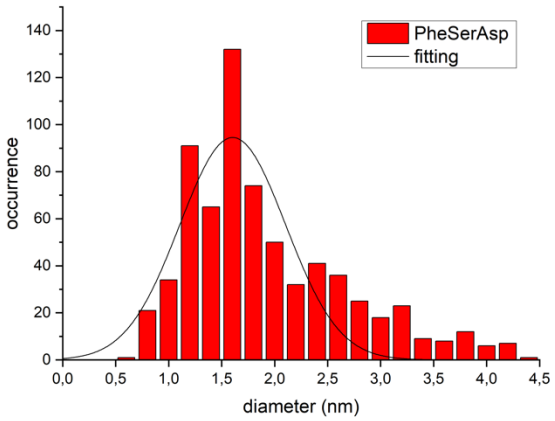

Figure S20. Sizing of PheSerAsp-AuNP, average diameter = 1.4 ± 0.6 nm, average cluster formula: $Au_{85}SR_{14}$.

Characterization of GlyIleAsp-AuNP

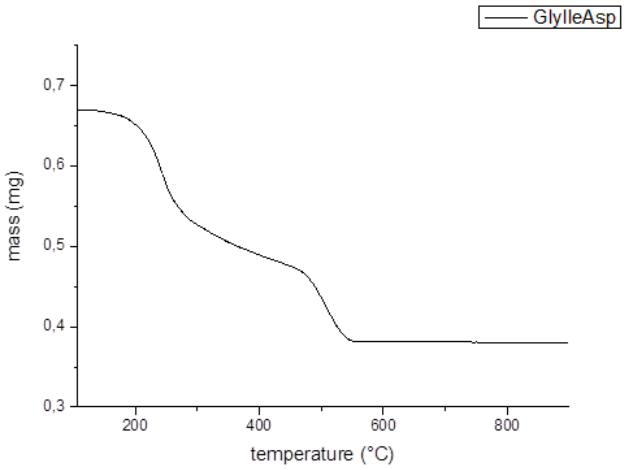

Figure S21. TGA analysis of GlyIleAsp-AuNP, weight loss = 57.03 %.

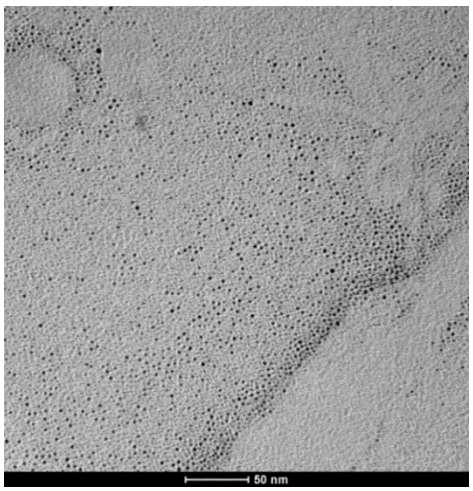

Figure S22. TEM analysis of GlyIleAsp-AuNP.

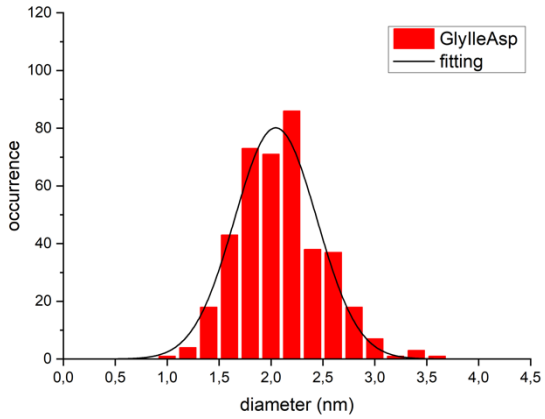

Figure S23. Sizing of GlyIleAsp-AuNP, average diameter = 1.8 ± 0.3 nm, average cluster formula: $Au_{180}SR_{84}$.

Characterization of ProProAsp-AuNP

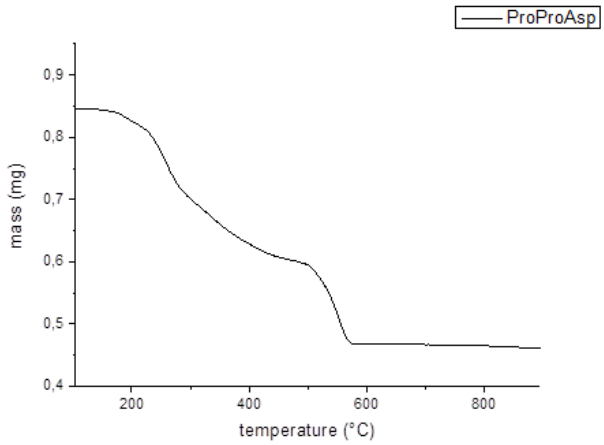

Figure S24. TGA analysis of ProProAsp-AuNP, weight loss = 55.24 %.

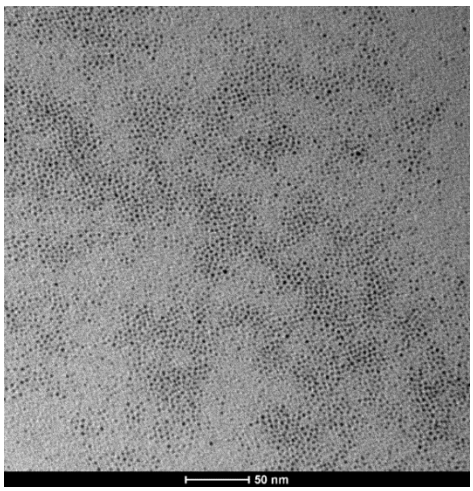

Figure S25. TEM analysis of ProProAsp-AuNP.

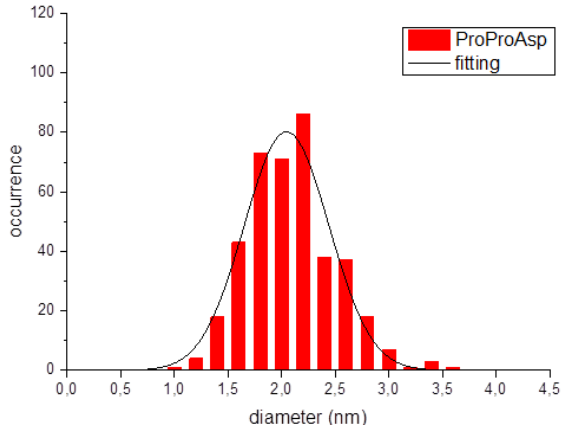

Figure S26. Sizing of ProProAsp-AuNP, average diameter = 2.0 ± 1.0 nm, average cluster formula: $Au_{247}SR_{107}$.

Characterization of PheLeuAsp-AuNP

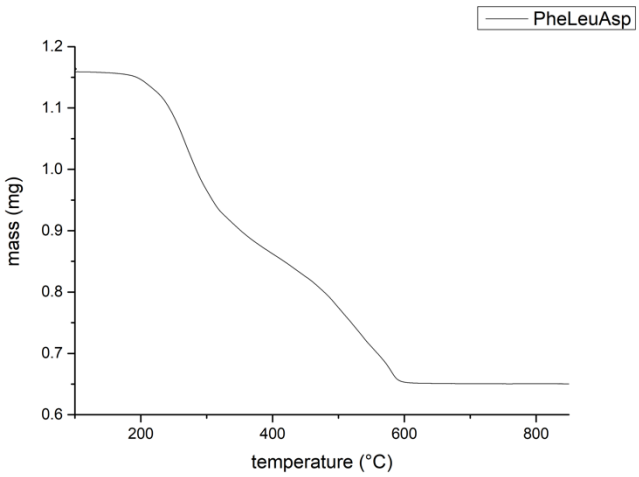

Figure S27. TGA analysis of PheLeuAsp-AuNP**,** weight loss = 44.28 %.

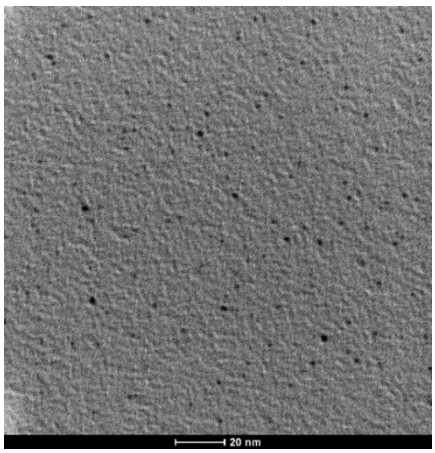

Figure S28. TEM analysis of PheLeuAsp-AuNP.

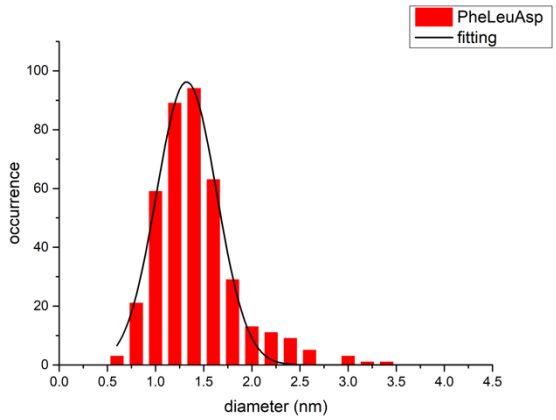

Figure S29. Sizing of PheLeuAsp-AuNP, diameter = 1.3 ± 0.3 nm, average cluster formula: $Au_{72}SR_{20}$.

Characterization of LeuLeuAsp-AuNP

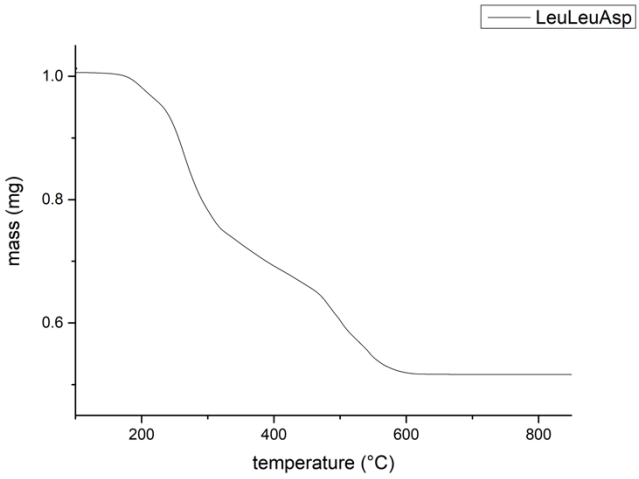

Figure S30. TGA analysis of LeuLeuAsp-AuNP**,** weight loss = 49.15 %.

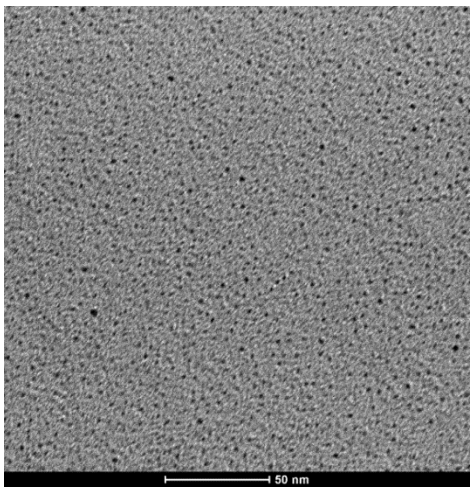

Figure S31. TEM analysis of LeuLeuAsp-AuNP.

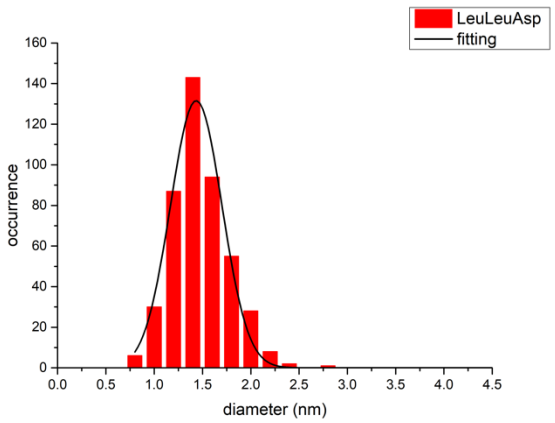

Figure S32. Sizing of LeuLeuAsp-AuNP, diameter = 1.4 ± 0.3 nm, average cluster formula: $Au_{91}SR_{33}$.

Characterization of TrpGlnAsp-AuNP

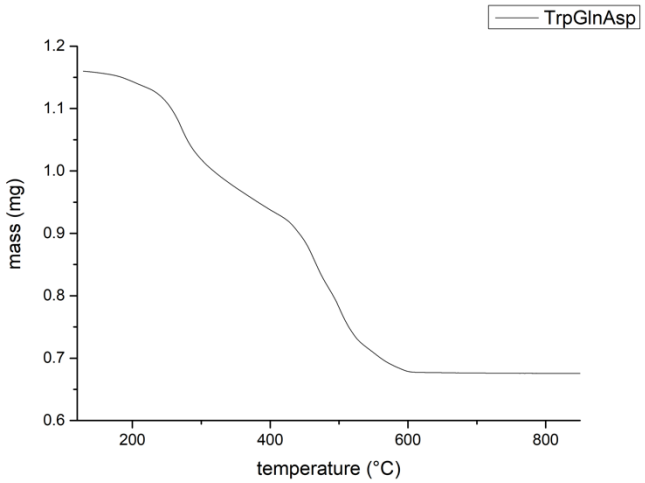

Figure S33. TGA analysis of TrpGlnAsp-AuNP, weight loss = 44.06 %.

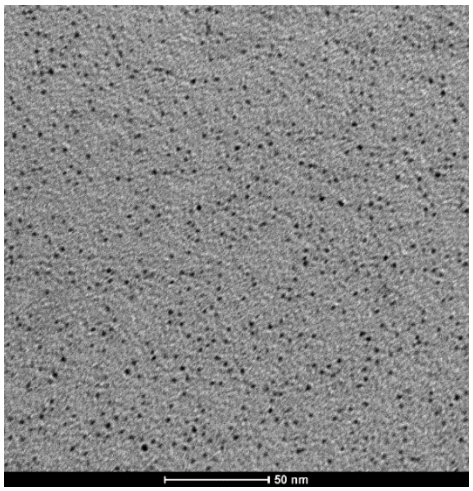

Figure S34. TEM analysis of TrpGlnAsp-AuNP.

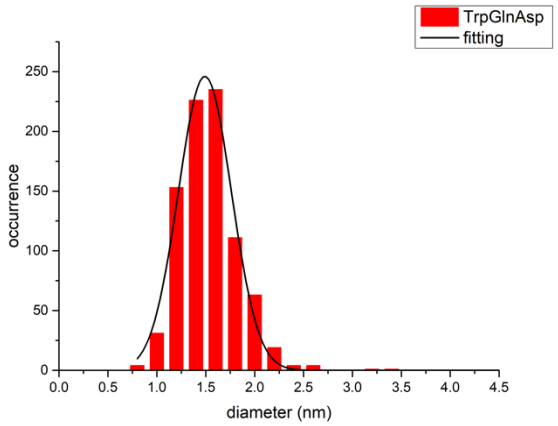

Figure S35. Sizing of TrpGlnAsp-AuNP**,** diameter = 1.5 ± 0.3 nm, average cluster formula: $Au_{102}SR_{26}$.

Characterization of ProAlaAsp-AuNP

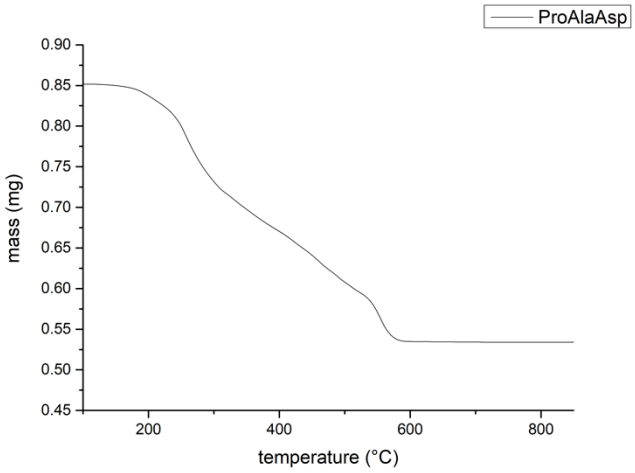

Figure S36. TGA analysis of ProAlaAsp-AuNP, weight loss = 37.27 %.

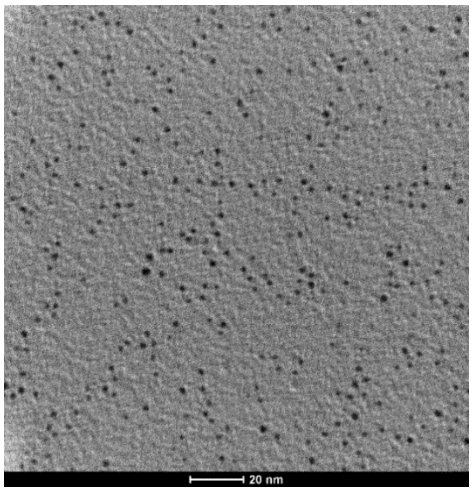

Figure S37. TEM analysis of ProAlaAsp-AuNP.

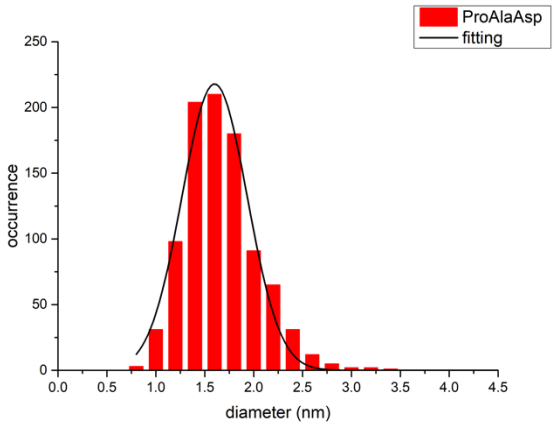

Figure S38. Sizing of ProAlaAsp-AuNP, diameter = 1.6 ± 0.3 nm, average cluster formula: $Au_{127}SR_{31}$.

Characterization of GlnGlnAsp-AuNP

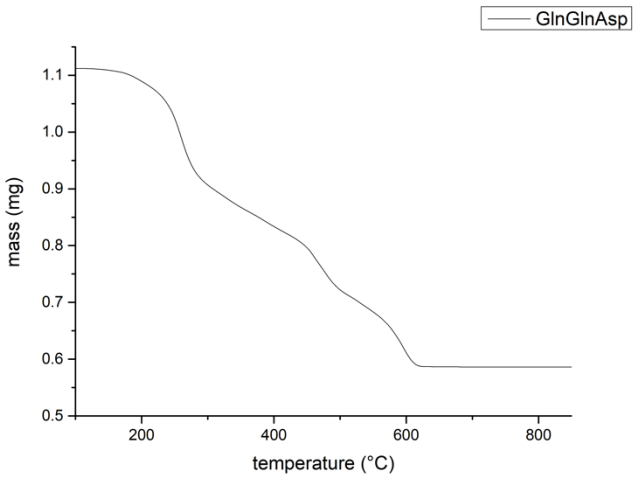

Figure S39. TGA analysis of GlnGlnAsp-AuNP, weight loss = 47.27 %.

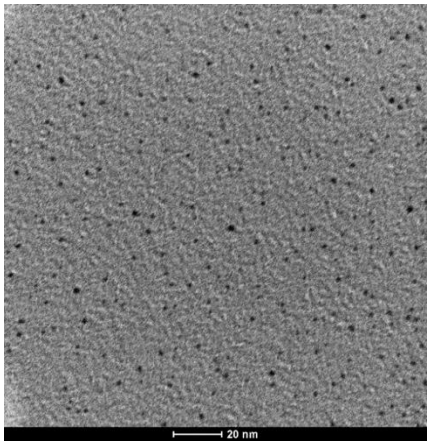

Figure S40. TEM analysis of GlnGlnAsp-AuNP.

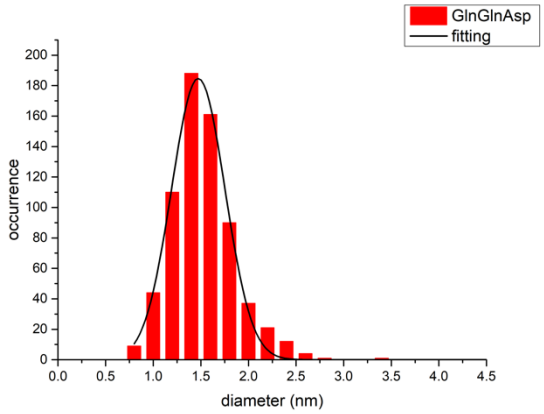

Figure S41. Sizing of GlnGlnAsp-AuNP, diameter = 1.5 ± 0.3 nm, average cluster formula: $Au_{99}SR_{31}$.

Characterization of GlnAlaAsp-AuNP

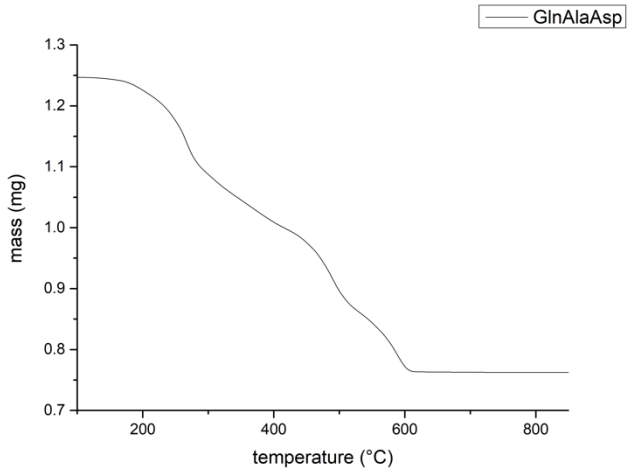

Figure S42. TGA analysis of GlnAlaAsp-AuNP, weight loss = 38.83 %.

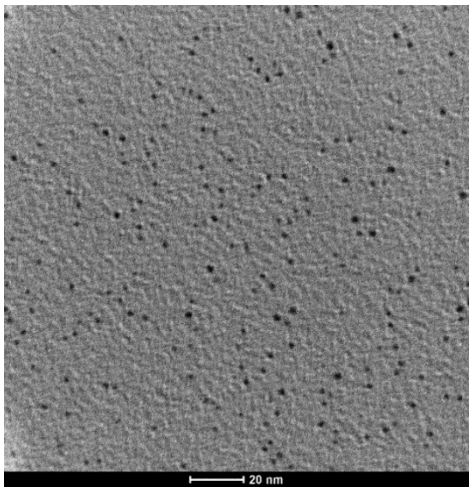

Figure S43. TEM analysis of GlnAlaAsp-AuNP.

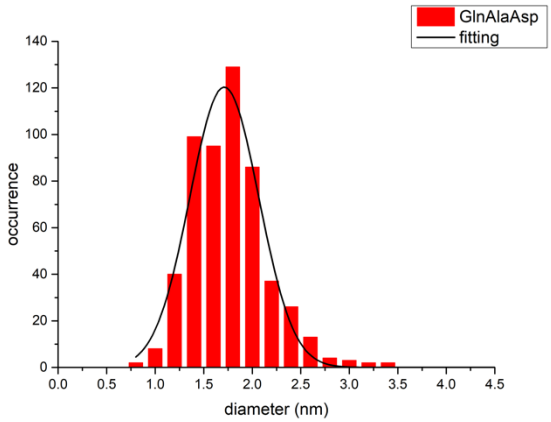

Figure S44. Sizing of GlnAlaAsp-AuNP, diameter = 1.7 ± 0.4 nm, average cluster formula: $Au_{155}SR_{39}$.

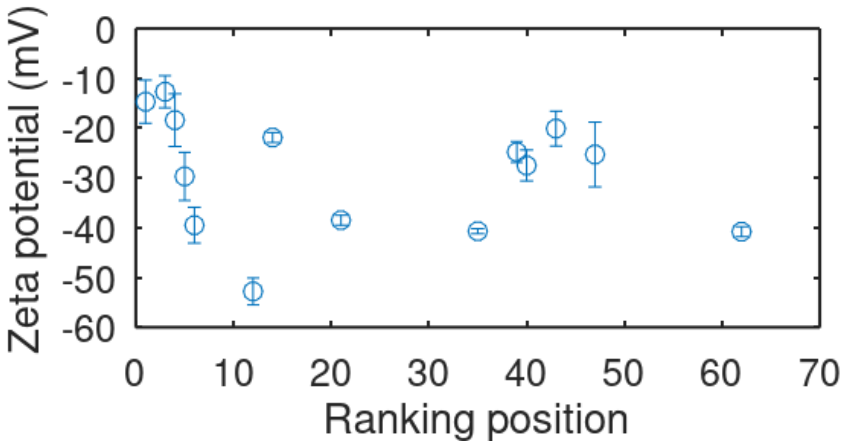

Figure S45. ζ-potential values vs ranking for the 10 AuNPs selected for experimental testing ([AuNP] = 0.01 mM, HEPES 1 mM). The correspondence between rank and AuNP is: 1 / TrpPheAsp-AuNP, 3 / GlnProAsp-AuNP, 4 / TyrProAsp-AuNP, 5 / TrpProAsp-AuNP, 6 / ProLeuAsp-AuNP, 12 / GlyIleAsp-AuNP, 14 / GlnGlnAsp-AuNP, 21 / PheSerAsp-AuNP, 35 / ProProAsp-AuNP, 39 / TrpGlnAsp-AuNP, 40 / LeuLeuAsp-AuNP, 43 / ProAlaAsp-AuNP, 47 / GlnAlaAsp-AuNP, 62/ PheLeuAsp-AuNP.

Additional NMR Spectra

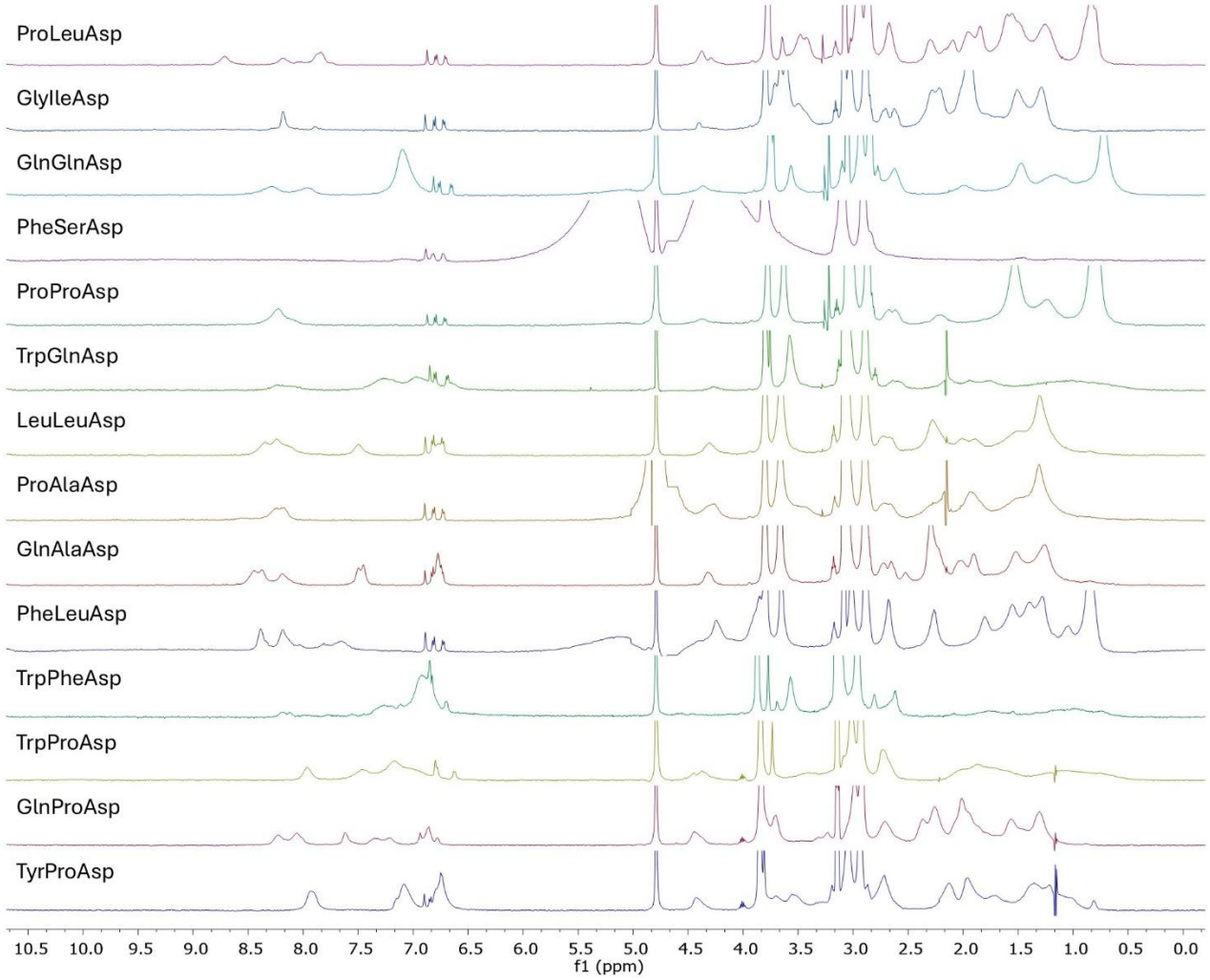

Figure S46. HPwSTD spectra of [3-MT] = 100 µM + [AuNP] = 500 µM (500 MHz, 25 °C, [HEPES] = 1 mM, pD = 7.0, H_2O/D_2O 90:10, 512 scans).

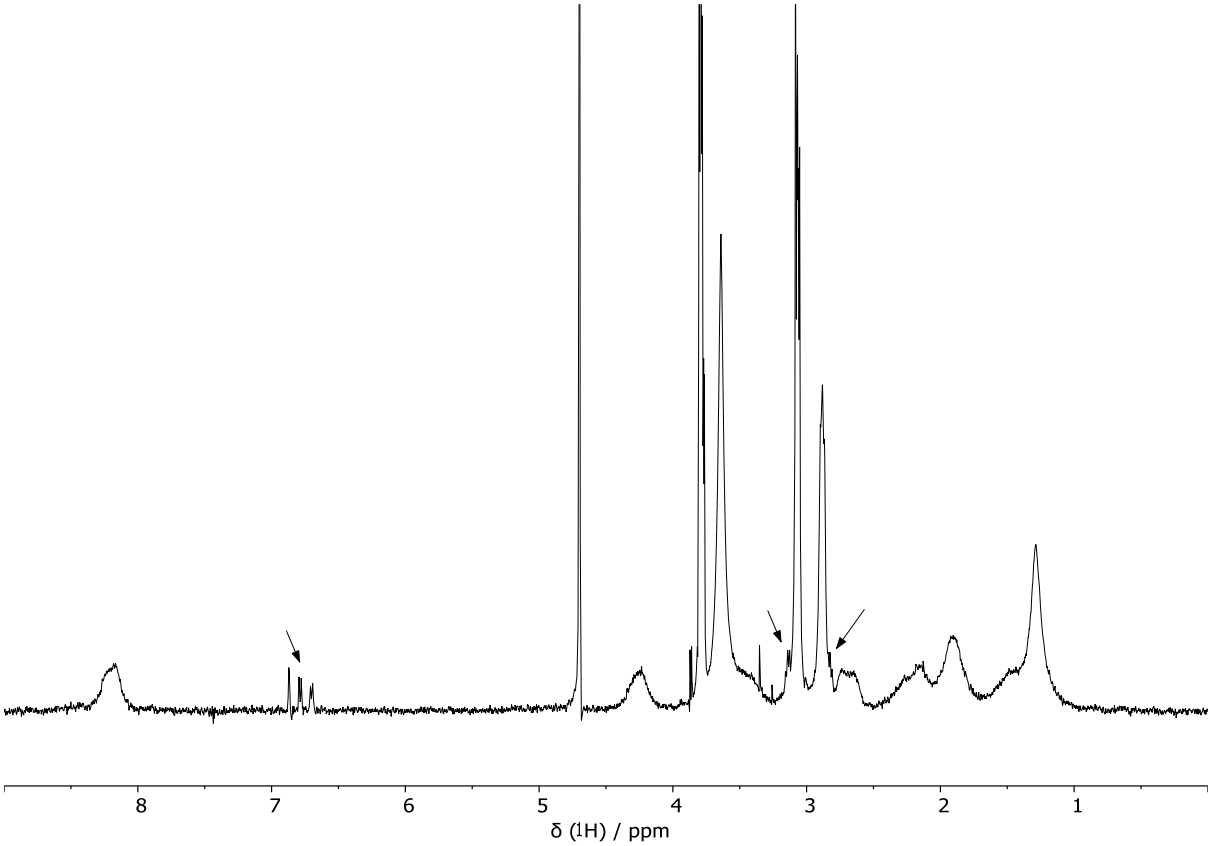

Figure S47. HPwSTD full spectrum of ProAlaAsp-AuNP 500 uM + 3-MT 50 uM + hippuric acid 50 uM + homovanillic acid 50 uM + vanillic acid 50 uM + 1 mM HEPES. The arrows indicate the signals of 3-MT. The signal of the ProAlaAsp-AuNP was attenuated by means of a 16 ms T_2-filter implemented into the W5 cluster.

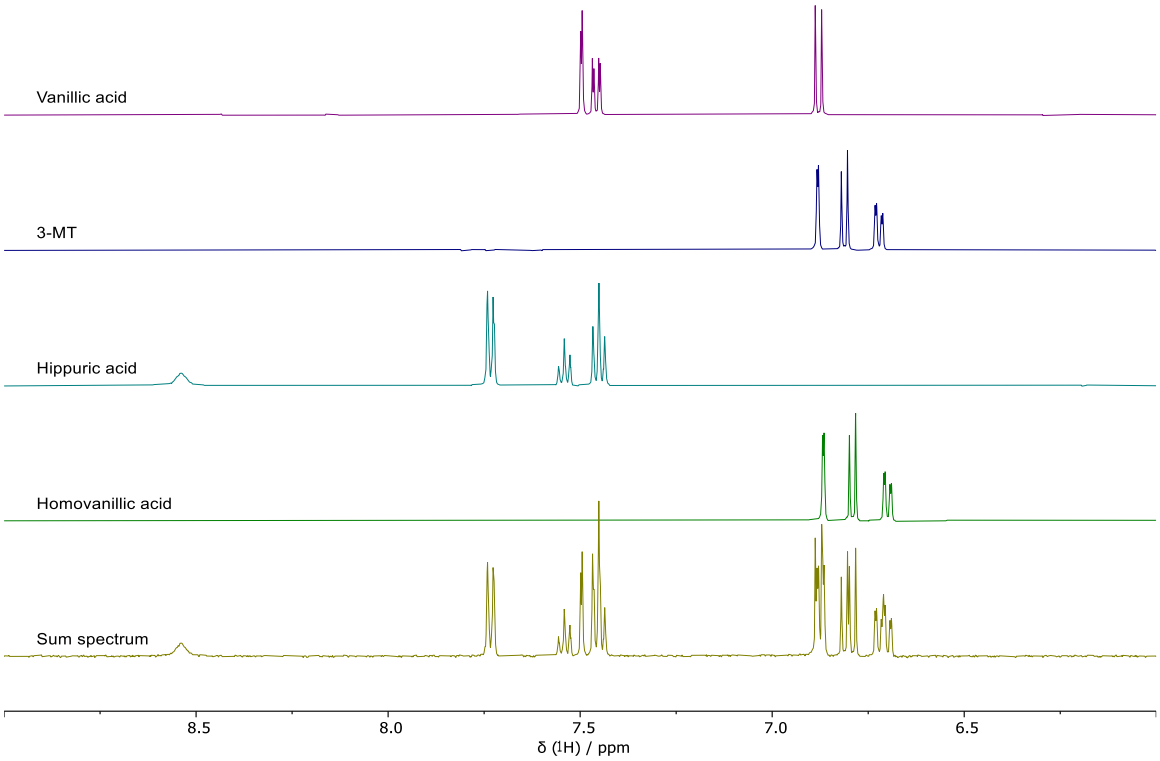

Figure S48. ^{1}H sub-spectra of standard analytes in 1 mM HEPES. The bottom spectrum is the sum of the above spectra.

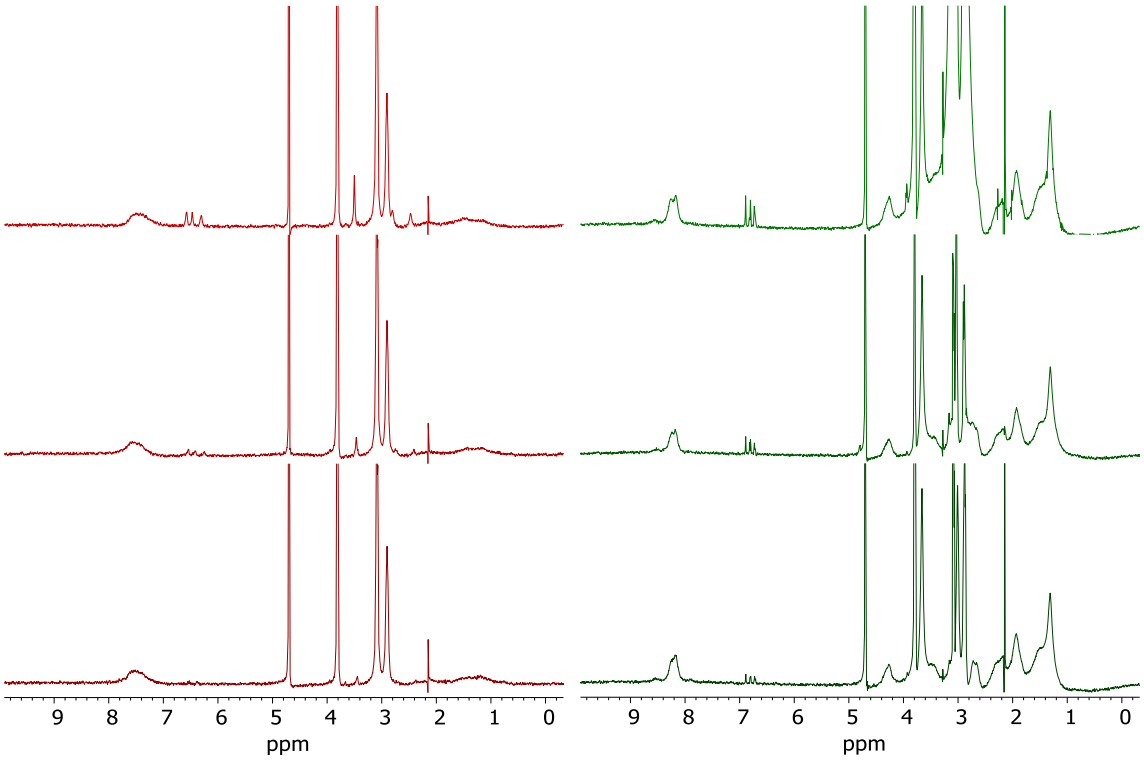

Figure S49. HPwSTD spectra of SO_3-AuNP (left) or ProAlaAsp-AuNP (right) at 500 µM + [3-MT] = 25-100 µM (500 MHz, 25 °C, [HEPES] = 1 mM, pD = 7.0, H_2O/D_2O 90:10, 512 scans).

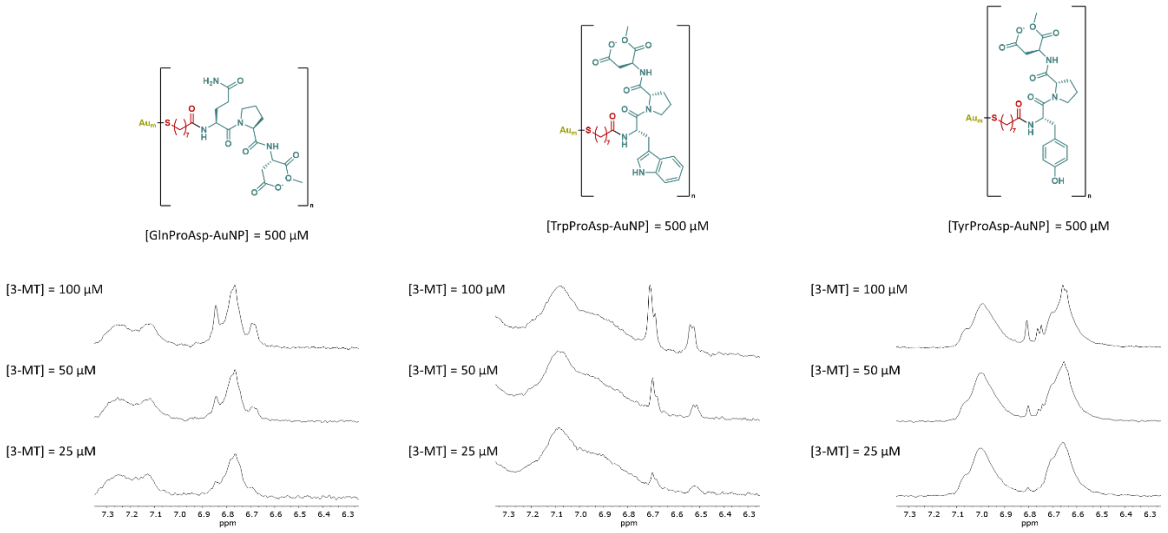

Figure S50. HPwSTD spectra of SO_3-AuNP (left) or ProAlaAsp-AuNP (right) at 500 µM + [3-MT] = 25-100 µM (500 MHz, 25 °C, [HEPES] = 1 mM, pD = 7.0, H_2O/D_2O 90:10, 512 scans).

Supplementary References

[1] S. Franco-Ulloa, L. Riccardi, F. Rimembrana, M. Pini, M. De Vivo, *J Chem Theory Comput* **2019**, *15*, 2022–2032.

[2] S. Franco-Ulloa, L. Riccardi, F. Rimembrana, E. Grottin, M. Pini, M. De Vivo, *J Chem Theory Comput* **2023**, *19*, 1582–1591.

[3] H. Heinz, R. A. Vaia, B. L. Farmer, R. R. Naik, *The Journal of Physical Chemistry C* **2008**, *112*, 17281–17290.

[4] E. Pohjolainen, X. Chen, S. Malola, G. Groenhof, H. Häkkinen, *J Chem Theory Comput* **2016**, *12*, 1342–1350.

[5] M. H. M. Olsson, C. R. Søndergaard, M. Rostkowski, J. H. Jensen, *J Chem Theory Comput* **2011**, *7*, 525–537.

[6] C. I. Bayly, P. Cieplak, W. Cornell, P. A. Kollman, *J Phys Chem* **1993**, *97*, 10269–10280.

[7] J. Wang, R. M. Wolf, J. W. Caldwell, P. A. Kollman, D. A. Case, *J Comput Chem* **2004**, *25*, 1157–1174.

[8] L. Gabrielli, D. Rosa-Gastaldo, M.-V. Salvia, S. Springhetti, F. Rastrelli, F. Mancin, *Chem Sci* **2018**, *9*, 4777–4784.

[9] W. L. Jorgensen, J. Chandrasekhar, J. D. Madura, R. W. Impey, M. L. Klein, *J Chem Phys* **1983**, *79*, 926–935.

[10] B. Hess, H. Bekker, H. J. C. Berendsen, J. G. E. M. Fraaije, *J Comput Chem* **1997**, *18*, 1463–1472.

[11] T. Darden, D. York, L. Pedersen, *J Chem Phys* **1993**, *98*, 10089–10092.

[12] B. Hess, C. Kutzner, D. van der Spoel, E. Lindahl, *J Chem Theory Comput* **2008**, *4*, 435–447.

[13] N. Michaud-Agrawal, E. J. Denning, T. B. Woolf, O. Beckstein, *J Comput Chem* **2011**, *32*, 2319–2327.

[14] F. De Biasi, D. Rosa-Gastaldo, X. Sun, F. Mancin, F. Rastrelli, *J Am Chem Soc* **2019**, *141*, 4870–4877.

[15] X. Sun, P. Liu, F. Mancin, *Analyst* **2018**, *143*, 5754–5763.

[16] X. Sun, L. Riccardi, F. De Biasi, F. Rastrelli, M. De Vivo, F. Mancin, *Angewandte Chemie International Edition* **2019**, *58*, 7702–7707.

[17] B. Perrone, S. Springhetti, F. Ramadori, F. Rastrelli, F. Mancin, *J Am Chem Soc* **2013**, *135*, 11768–11771.